



Technical Document 2940
January 1997

Radar Target Detection in Wideband Clutter and Noise Closed-Form Detection Algorithms for Radar System Modeling

R. H. Ott D. R. Wehner R. J. Dinger
GRCl, Inc. QuesTech, Inc. NRaD

Naval Command, Control and
Ocean Surveillance Center
RDT&E Division

San Diego, CA
92152-5001

19970304 024



Approved for public release; distribution is unlimited.

The views and conclusions contained in this report are those of the contractors and should not be interpreted as representing the official policies, either expressed or implied, of the Naval Command, Control and Ocean Surveillance Center RDT&E Division or the U.S. Government.

DTIC QUALITY INSPECTED 1

Technical Document 2940

January 1997

**Radar Target Detection in
Wideband Clutter and Noise
Closed-Form Detection
Algorithms for Radar
System Modeling**

R. H. Ott, GRCI, Inc.
D. R. Wehner, QuesTech, Inc.
R. J. Dinger, NRaD

**NAVAL COMMAND, CONTROL AND
OCEAN SURVEILLANCE CENTER
RDT&E DIVISION
San Diego, California 92152-5001**

**H. A. WILLIAMS, CAPT, USN
Commanding Officer**

**DR. R. C. KOLB
Executive Director**

ADMINISTRATIVE INFORMATION

The work detailed in this report was performed for the Naval Command, Control and Ocean Surveillance Center (NCCOSC) RDT&E Division (NRaD), under program element 0602232N, Contract N66001-D-94-0009, by QuesTech, Inc., 1011 Camino del Rio South, Suite 600, San Diego, CA 92108 and GRCI, Inc., 3900 Juan Tabo Boulevard, NE, Suite 12, Albuquerque, NM 87111-3984. R. J. Dinger, Radar Branch Head, Code D755, was the technical coordinator for the project.

Released by
R. J. Dinger, Head
Radar Branch

Under authority of
J. E. Griffin, Head
Electromagnetic/
Electro-Optic Division

Authorship

Mr. Don Wehner, formerly the radar branch chief, NRaD, code 755, formulated the problem and described the requirements. Dr. Randy Ott developed the mathematics.

Objective

This work derived the mathematics required in the RSCEM (Radar Simulation Concept Evaluation Model) model for closed-form answers for the probability of detection and false alarm for Swerling class targets in clutter and noise and targets in compound-K clutter plus noise. In all cases, the results are applicable to the N-pulse coherent detection problem. For the case of a target in "spikey" clutter plus the noise the advantage of multiple pulse integration is significant.

Funding was provided under contract #N66001-94-D-0009.

Table of Contents

section	page
1. Introduction	6
2. Probability Density Functions for a Target in Clutter and Noise	
2.1 General Case	7
2.2 Swerling Case #0	15
2.3 Swerling Case #1	20
2.4 Swerling Case #2	25
2.5 Swerling Case #3	29
2.6 Swerling Case #4	36
2.7 Swerling target plus compound-k clutter and Gaussian noise.	40
3. An Alternative Derivation for Swerling Case #2 target, $N=1$	49
4. Probability Density function for Broad-Band Clutter constant pulse-to-pulse but varying scan-to-scan (no target)	54
5. References	63
6. Computer Code	65

List of Figures

Figure	page
1) Phasor diagram for a target in clutter plus noise	7
2) Various Swerling class time series representations for a fluctuating target	14
3) Probability of detection versus signal-to-noise ratio for a Swerling case # 0 target. $N=1, 2$.	19
4) Probability of detection versus signal-to-noise ratio for a Swerling case # 1 target. $N=1, 2, 3, \dots, 10$.	24
5) Probability of detection versus signal-to-noise ratio for a Swerling case # 2 target. $N=1, 2$.	28
6) Probability of detection versus signal-to-noise ratio for a Swerling case # 3 target. $N=1, 2, 3$.	35
7) Probability of detection versus signal-to-noise ratio for a Swerling case # 4 target. $N=1, 2, 3$.	39
8) Probability of detection versus signal-to-noise ratio for a target in spikey clutter and noise. $N=1, 2, 3$.	45
9) Probability of detection versus signal-to-noise ratio for a Swerling case # 2 target, for three different false alarm ratios.	52
10) A comparison of the compound-K and Rayleigh pdf's.	58
11) A Comparison of the approximate compound-K and Rayleigh pdf's	60

1. Introduction

Target detection in Gaussian noise is an old problem and there too many references to cite them all here. Similarly, there are several published results for target detection in Gaussian noise and log-normal clutter (Trunk and George, 1970, Schleher, 1975). Although some of the analysis in this report is derived elsewhere, we have tried to present a unified approach to the problem of target detection in clutter plus noise to include all the standard Swerling target cases and the relatively new compound-K clutter probability density function, as discussed by Ward et al.(1990). In the following analysis, many of the derivations are new and yield closed form results for the N-pulse case for the probability of detection, and probability of false alarm for Swerling class targets in Gaussian noise, assuming square-law detection. All the derivations are not new; however, to the authors knowledge, they do not appear in a single reference for all combinations of Swerling targets and clutter statistics, including compound-k. The report considers the following theoretical problems:

1) The use of the characteristic function to treat the problem of N-multiple pulse integration, for SC-0, SC-1, SC-2, SC-3, SC-4 and compound-k clutter cases.

2) The use of a basic rule in probability theory for removing "left" and "right" variables in conditional pdf's to treat the problem of target plus clutter in noise, and then target in clutter, in place of multiple convolutions of the individual pdf's representing the sum of the random variables target, clutter and noise.

3) The use of the recently reported compound-K pdf for treating "spikey" clutter arising in wide-band radar applications.

4) FORTRAN 77 algorithms for all Swerling cases for target plus noise, and Swerling case #1 and #2 targets in compound-k clutter.

2. Probability Density Functions for a Target in Clutter and Noise

2.1 General Case

A detection decision is to be made during each N-pulse beam-dwell interval. In the general case, the target and the clutter can vary from pulse-to-pulse and from scan-to-scan. An extension of the usual two-components representing the complex phasors for the I and Q output of the received signal to include clutter, after post detection is the following three component model

$$\mathbf{Re}^{i\theta} = \tau e^{i\omega} + \gamma e^{i\varsigma} + re^{i\phi}, \quad (1)$$

where $\tau e^{i\omega}$ is the complex phasor representing the target, $\gamma e^{i\varsigma}$ is the complex phasor representing the clutter, and $re^{i\phi}$ is the complex phasor representing thermal noise. A vector diagram for the three phasors is shown in figure 1, where the detection is made on the basis of $|\mathbf{Re}^{i\theta}|$ in equation (1). Note, the symbol ω in equation (1) should not be confused with the same parameter when used in the characteristic function.

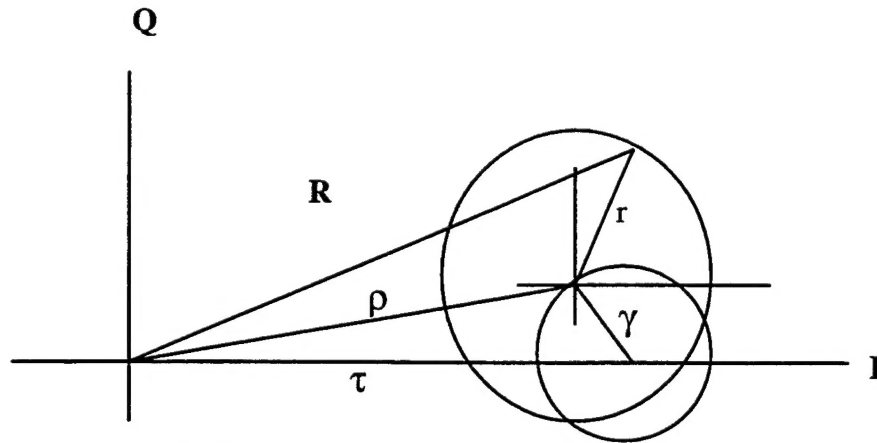


Figure 1. Phasor diagram for three components of the received signal.

If the target is immersed in Gaussian noise and clutter, and this target is to be detected using an N-pulse radar burst, the return can in equation (1) can be written as

$$\mathbf{Re}^{i\theta} = \rho e^{i\psi} + re^{i\phi}, \quad (2)$$

where the target plus clutter is decomposed as

$$\rho e^{i\psi} = \tau e^{i\omega} + \gamma e^{i\zeta} . \quad (3)$$

The pdf for the return, $\mathbf{R}e^{i\theta}$, can be written, using the basic rule; to remove a number of “left” variables, we integrate with respect to them. To remove a number of “right” variables, we multiply by their conditional density with respect to the remaining “right” variables and integrate (Papoulis, 1965, p.236). For example, for two “right” removals we have,

$$p(x_1|x_4) = \iint_{-\infty}^{\infty} p(x_1|x_2, x_3, x_4) p(x_2, x_3|x_4) dx_2 dx_3 . \quad (4)$$

For the case of a target in noise alone (no clutter in equation (1)) standard Swerling cases use a Rayleigh pdf for the noise component given by

$$p_n(r) = \frac{r}{\sigma_n^2} e^{-\frac{r^2}{2\sigma_n^2}} . \quad (5)$$

The distribution of R in equation(1) with no clutter; i.e., where $\rho e^{i\psi} = \tau e^{i\omega}$ is Rice given by

$$p(R|\rho) = \frac{R}{\sigma_n^2} e^{-(R^2+\rho^2)/2\sigma_n^2} I_0\left(\frac{R\rho}{\sigma_n^2}\right) . \quad (6)$$

Assume a square-law detector. The actual detector type; i.e., linear, half-wave, square-law, full-wave square-law introduces only minor differences in the correlation function of the received signal, i.e., all correlation outputs are proportional to the mean square received power with second order differences depending on the time shift. Make the following substitutions:

$$y = \frac{R^2 / 2}{\sigma_n^2}, \quad dy = \frac{RdR}{\sigma_n^2},$$

$$x = \frac{\rho^2 / 2}{\sigma_n^2}, \quad (7)$$

and temporarily treat ρ as though it were a constant, and R is the detected amplitude. Substituting equation (7) into equation (6) gives, for each pulse, in the SC-0, SC-1, SC-2, SC-3, and SC-4 cases,

$$p(y|x) = \begin{cases} e^{-(x+y)} I_0(2\sqrt{xy}), & y \geq 0 \\ 0 & , y < 0 \end{cases}, \quad (8)$$

where the pdf in equation (8) is conditioned on x . DiFranco and Rubin (p.370, 1980) show that there is negligible difference in detection performance (as measured in terms of the probability density function) between a square-law envelope detector and a linear detector (on the order of 0.1 dB). Blake (p.44, 1986) also states the difference between square-law and linear detection in terms of the required signal-to-noise ratio for detection is on the order of 0.2dB at most. As a point of interest, the result in equation (8) can be shown to be equivalent to the result in Nathanson.¹

¹ second edition (p. 168, Table 5.6, entry (5), Rice (power), 1991), by making the following substitutions in equation (8)

$$y = (1 + a^2)x$$

$$\rho = a\sqrt{x}$$

$$y = \frac{R^2 / 2}{\sigma_n^2}, \quad x = \frac{\rho^2 / 2}{\sigma_n^2}$$

where a^2 is the ratio of the large reflection (target) to the sum of small reflections (clutter), x is the rcs, and $\bar{x} = 2\sigma_n^2$ is the mean rcs. We note a "typo" in Nathanson, where the density function for the rcs, x , should read in the argument of the Bessel function as

$$J_0 \left[2ia \sqrt{(1 + a^2) \left(\frac{x}{\bar{x}} \right)} \right] = I_0(2\sqrt{xy})$$

In order to treat the case of multiple pulse post-detection integration gain efficiency, it is convenient to introduce the characteristic function associated with $p(y|x)$ in equation (8) as

$$\Phi(\omega|x) = \int_{-\infty}^{\infty} p(y|x) e^{i\omega y} dy, \quad (9)$$

and substituting equation (8) into equation (9) gives

$$\begin{aligned} \Phi(\omega|x) &= e^{-x} \int_0^{\infty} e^{-y(1-i\omega)} I_0(2\sqrt{xy}) dy \\ &= e^{-x} \frac{e^{\frac{x}{(1-i\omega)}}}{(1-i\omega)} \\ &= \frac{e^{-\left(x \frac{x}{1-i\omega}\right)}}{1-i\omega} \end{aligned} \quad (10)$$

We will now consider the N-pulse detection case. For N-pulse detection, we detect the sum of N different values, y_1, \dots, y_N of the received power and noise as

$$\begin{aligned} Y &= y_1 + y_2 + \dots + y_N, \\ &= \left(\frac{R_1^2 / 2}{\sigma_n^2} \right) + \left(\frac{R_2^2 / 2}{\sigma_n^2} \right) + \dots + \left(\frac{R_N^2 / 2}{\sigma_n^2} \right) \\ &= \frac{|\rho + r_1 e^{i\phi_1}|^2}{2\sigma_n^2} + \frac{|\rho + r_2 e^{i\phi_2}|^2}{2\sigma_n^2} + \dots, \end{aligned} \quad (11)$$

$$Exp\{Y|x\} = N \frac{\rho^2 / 2}{\sigma_n^2} + N = Nx + N = N(x + 1)$$

where the last line in equation (11) will be obtained by an alternative method shortly, and X is defined in equation (7).

If the pulse-to-pulse noise samples are statistically independent, then the characteristic function of the sum of the N samples is the produce of their individual characteristic functions. Therefore, the characteristic function associated with Y is

$$\Phi_N(\omega|x) = \frac{e^{-N\left(x\frac{\omega}{1-i\omega}\right)}}{(1-i\omega)^N}. \quad (12)$$

A slight modification of the order of first averaging over $p(x)$ and next taking the product of the individual characteristic functions is required for SC-4. In this case we need to average with respect to one-dominant-scatter plus Rayleigh noise, before finding the sum of the N samples. The advantage of performing the multiple pulse analysis in the "frequency" domain as in equation (12) as opposed to the probability domain is that the expression corresponding to (12) in the pdf domain is an N -fold convolution of each of the N pdf's for each of the N variables.

Now, because the target plus clutter fluctuates from scan-to-scan, for all Swerling class targets, we must average equation (10) over the variable $x = \frac{\rho^2}{2\sigma_n^2}$. That is,

$$\begin{aligned} \Phi_N(\omega) &= \int_{-\infty}^{\infty} \Phi_N(\omega|x) p(x) dx \\ &= \int_{-\infty}^{\infty} [\Phi(\omega|x)]^N p(x) dx, \\ &= \frac{1}{(1-i\omega)^N} \int_{-\infty}^{\infty} e^{-N\left(x\frac{\omega}{1-i\omega}\right)} p(x) dx \end{aligned} \quad (13)$$

where $p(x)$ is the probability density function for the random variable X . In the case of Swerling class targets, $p(x)$ corresponds to the density function of the target alone, appropriate to either pulse-to-pulse variation or scan-to-scan variation. For the case of target plus clutter plus noise, a similar analysis will be used as shown in section 2.7. In the case of Swerling class targets, once $\Phi_N(\omega)$ is known, the probability density of $Y = y_1 + y_2 + \dots + y_N$, the desired result, is

$$p_N(Y) = \frac{1}{2\pi} \int_{-\infty}^{\infty} \Phi_N(\omega) e^{-i\omega Y} d\omega \quad (14)$$

Equations (13) and (14) are extremely useful, and form a “key pair” and will be used in several of the following derivations.

Before leaving the subject of the characteristic function associated with a pdf it is instructive to consider the meaning of the parameter ω^2 in the definition for the characteristic function. First, this parameter is a dummy variable of integration. Second, it is not really frequency, but simply a variable used to analytically continue the characteristic function into the complex plane in order to consider the moments of the random variable. The derivatives of the characteristic function of a random variable, Y , are related to its moments as

$$\text{Exp}\{Y^n|x\} = \frac{1}{i^n} \left. \frac{d^n \Phi}{d\omega^n} \right|_{\omega=0}, \quad (15)$$

and the Taylor's series expansion (a Laurent series is a more general analytic continuation for a function of a complex variable) for the characteristic function is

$$\Phi(\omega|x) = 1 + i\omega m_1 - \omega^2 m_2 + \cdots + \frac{(i\omega)^n}{n!} m_n + \cdots \quad (16)$$

For the characteristic function given in equation (16) we find for the first two derivatives

² See remark on page 6.

$$\begin{aligned}
\frac{d\Phi}{d\omega} &= \int_0^{\infty} \frac{e^{\frac{i\omega Nx}{1-i\omega}}}{(1-i\omega)^{N+1}} \left[iN + iNx - \frac{N\omega x}{1-i\omega} \right] p(x) dx \\
\left. \frac{d\Phi}{d\omega} \right|_{\omega=0} &= iN \int_0^{\infty} (1+x) p(x) dx \\
\left. \frac{d^2\Phi}{d\omega^2} \right|_{\omega=0} &= -N \int_0^{\infty} xp(x) dx + iN \int_0^{\infty} (iN + iNx) p(x) dx
\end{aligned} \tag{17}$$

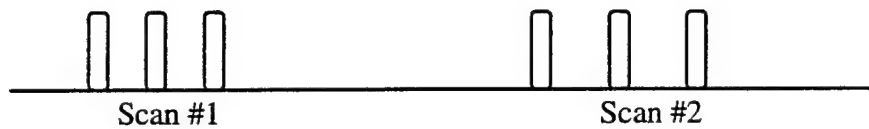
and from the second line in equation (17) we see

$$\text{Exp}\{Y|x\} = N(x+1), \tag{18}$$

which is the same statement as equation (11) as of course it must be. It is also easy to show that

$$\begin{aligned}
\frac{d^2\Phi}{d\omega^2} &= -N[1 + 2(x+n+Nx)] \\
\sigma_Y^2 &= \text{Exp}\{Y^2\} - (\text{Exp}\{Y\})^2 \\
&= 3N
\end{aligned} \tag{19}$$

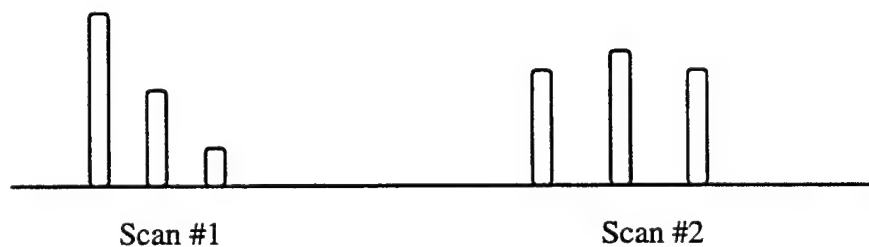
Before considering the various Swerling cases, it is instructive to draw a picture of target echo's varying on either a pulse-to-pulse or a scan-to-scan basis. Hopefully, such a picture helps explain the choice for a particular pdf used in the following sections. Figure 2 shows a time series (or equivalently, a range profile) of received echo fluctuations under different circumstances.



SC-0: Steady target.



SC-1 and SC-3: Steady target pulse-to-pulse.



SC-2 and SC-4: Pulse-to-pulse variation. For SC-4, there is a dominant pulse in each scan.

Fig.2 Various Swerling class time series representations for a fluctuating target.

2.2 Swerling Case #0 (non-fluctuating target):

In this case, we see from figure 2, that the target is constant pulse-to-pulse and scan-to-scan, and the total received signal can be written as

$$\text{Re}^{i\vartheta} = \frac{A^2 / 2}{\sigma_n^2} + r e^{i\varphi}, \quad (20)$$

where

$$\tau e^{i\omega} = \frac{A}{\sqrt{2}}, \quad (21)$$

and where the average target power to noise power is the first term on the right-hand-side of equation (20), and the phase is constant. This case was originally discussed by Marcum (1960). The pdf for the target in equation (20) is

$$p(x) = \delta\left(x - \frac{A^2 / 2}{\sigma_n^2}\right), \quad (22)$$

and substituting equation (22) into equation (13) gives

$$\Phi_N(\omega) = \frac{1}{(1 - i\omega)^N} e^{-N \frac{(A^2 / 2)}{\sigma_n^2} \left(\frac{-i\omega}{1 - i\omega} \right)}, \quad (23)$$

in agreement with Fehlner (1962, his equation A-4 on page 24). Substituting equation (23) into equation (14) of our “key pair” gives

$$P_N(Y) = \frac{1}{2\pi} \int_{-\infty}^{\infty} \frac{1}{(1-i\omega)^N} e^{\frac{i\omega Nb}{1-i\omega} - i\omega Y} d\omega$$

$$b = \frac{A^2 / 2}{\sigma_n^2}$$
(24)

We need to perform a bit of algebra to write the integral in equation (24) in “closed form,” a goal throughout this report.

$$1 - i\omega = iu, i\omega = 1 - iu$$

$$u = -i - \omega$$

$$du = -d\omega$$

$$p_N(Y) = \frac{e^{-(Y+Nb)}}{2\pi} \int_{-i-\infty}^{i+\infty} \frac{e^{i\left(uY - \frac{Nb}{u}\right)}}{(iu)^N} du$$
(25)

$$\xi = iu, d\xi = idu$$

$$p_N(Y) = \frac{e^{-(Y+Nb)}}{2\pi i} \int_{1-i\infty}^{1+i\infty} \frac{e^{\left(\xi Y + \frac{Nb}{\xi}\right)}}{\xi^N} d\xi$$

The last line in equation (25) is can be written in terms of a Laplace transform as

$$p_N(Y) = e^{-(Y+Nb)} \frac{1}{2\pi i} \int_{1-i\infty}^{1+i\infty} e^{\xi Y} \frac{e^{\frac{Nb}{\xi}}}{\xi^N} d\xi$$

$$= e^{-(Y+Nb)} \left(\frac{Y}{Nb}\right)^{\frac{N-1}{2}} I_{N-1}(2\sqrt{NbY})$$
(26)

where the last line in equation (26) follows from transform pair 29.3.81, page 1026, AMS55, Handbook of Mathematical Functions, National Bureau of Standards, 1964.

The probability of detection, for the N-pulse case, is then the simple numerical integration of equation (26) as

$$P_D = \int_{Y_o}^{\infty} p_N(Y) dY = e^{-Nb} \int_{Y_o}^{\infty} e^{-Y} \left(\frac{Y}{Nb} \right)^{\frac{N-1}{2}} I_{N-1}(2\sqrt{NbY}) dY \quad (27)$$

The probability of false alarm is found by setting $b = 0$ (N.B., this corresponds to setting x , the ratio of mean target power to noise variance to zero), and this is most easily accomplished in equation (25) since (26) is indeterminate. From (25) with $b = 0$ we find

$$\begin{aligned} p_N(Y, b = 0) &= \frac{e^{-Y}}{2\pi i} \int_{1-i\infty}^{1+i\infty} \frac{e^{\xi Y}}{\xi^N} d\xi \\ &= \frac{e^{-Y} Y^{N-1}}{(N-1)!} \end{aligned} \quad (28)$$

and the probability of false alarm becomes

$$\begin{aligned} P_{FA} &= \int_{Y_o}^{\infty} p_N(Y, b = 0) dY \\ &= \frac{1}{(N-1)!} \int_{Y_o}^{\infty} e^{-Y} Y^{N-1} dY \end{aligned} \quad (29)$$

which is easily evaluated by integration by parts.

For a $P_{FA} = 10^{-8}$ ($Y_o = 8 \times \log_e 10 \cong 18.42068$), and $N=1$,

$$P_D = 1 - e^{-b} \int_0^{Y_o} e^{-Y} I_0(2\sqrt{bY}) dY,$$

and for $N=2$,

$$P_D = 1 - e^{-2b} \int_0^{Y_o} e^{-Y} \left(\frac{Y}{2b} \right)^{\frac{1}{2}} I_1(2\sqrt{2bY}) dY,$$

and

$$P_{FA} = e^{-Y_o} (1 + Y_o),$$

and, for illustrative purposes, figure 3 shows a plot of P_D versus $\frac{A^2 / 2}{\sigma_n^2}$ in dB.

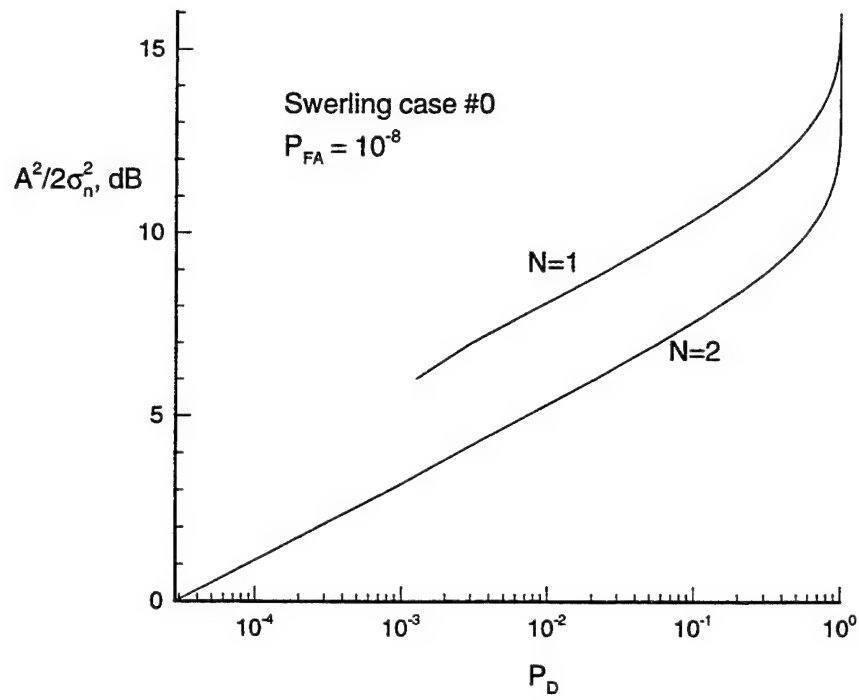


Fig. 3 Probability of detection versus signal-to-noise ratio for Swerling Case #0.

2.3 Swerling Case #1:

For both Swerling cases SC-1 and SC-3 we see from figure 2 that

$$\text{Re}^{i\theta} = \rho + re^{i\phi}, \quad (30)$$

where the first term on the right-hand-side of equation (30) fluctuates from scan-to-scan but is constant from pulse-to-pulse. The scan-to-scan Rayleigh pdf for the normalized mean target power for this case is

$$p(x') = e^{-x'}, \quad x' \geq 0, \quad (31)$$

or, in terms of the unnormalized mean power to noise variance, x_a ,

$$\begin{aligned} x' &= \frac{x}{x_a} = \frac{\rho^2 / 2}{x_a \sigma_n^2} = \frac{\rho^2 / 2}{\sigma_T^2} \\ x_a &= \frac{\sigma_T^2}{\sigma_n^2} \\ dx' &= \frac{1}{x_a} dx, \\ p(x) &= p(x') \frac{dx'}{dx} = \frac{e^{-\frac{x}{x_a}}}{x_a} \end{aligned} \quad (32)$$

and in going from x to x' there are two normalization's, first by x_a , and then the normalization used in the definition of x_a itself.

Before proceeding, we show that equation (32) is indeed a Rayleigh pdf, for the target voltage, ρ . From the definition of x ,

$$\begin{aligned}
x &= \frac{\rho^2 / 2}{\sigma_n^2}, dx = \frac{\rho}{\sigma_n^2} d\rho \\
p(\rho) &= p(x) \frac{dx}{d\rho} \\
&= \frac{\rho}{\sigma_n^2} e^{-\frac{\rho^2}{2\sigma_n^2}}
\end{aligned} \tag{33}$$

Substituting $p(x)$ from the last line of equation (32) into equation (13) gives

$$\begin{aligned}
\Phi_N(\omega) &= \frac{1}{(1-i\omega)^N} \frac{1}{x_a} \int_0^\infty e^{-x \left[\frac{1}{x_a} \frac{iN\omega}{1-i\omega} \right]} dx \\
&= \frac{1}{(1-i\omega)^{N-1} [1-i\omega(1+Nx_a)]}
\end{aligned} \tag{34}$$

Substituting equation (34) into equation (14) yields the probability density for the N-pulse case as

$$\begin{aligned}
p_N(Y) &= \frac{1}{2\pi} \frac{1}{(1+Nx_a)} \int_{-\infty}^\infty \frac{e^{-i\omega Y}}{(\omega_a - i\omega)(1-i\omega)^{N-1}} d\omega \\
\omega_a &= \frac{1}{1+Nx_a}
\end{aligned} \tag{35}$$

We now treat various values for N.

case N=1:

$$\begin{aligned}
P_1(Y) &= \frac{1}{2\pi} \frac{1}{(1+x_a)} \int_{-\infty}^{\infty} \frac{e^{-i\omega Y}}{(\omega_a - i\omega)} d\omega \\
&= \frac{e^{\frac{Y}{1+x_a}}}{1+x_a}
\end{aligned} \tag{36}$$

and the corresponding probability of detection is

$$P_D = \int_{Y_o}^{\infty} p_1(Y) dy = e^{\frac{Y_o}{1+x_a}}, \tag{37}$$

and $P_{FA} = e^{-Y_o}$ (from equation (36) with $x_a = 0$), and both 36 and 37 agree exactly with Fehlner (his equation 15, page 18).

N=2:

Expand the integrand in equation (35) using a partial fraction expansion as

$$\begin{aligned}
\frac{1}{(\omega_a - i\omega)(1 - i\omega)} &= \frac{A}{\omega_a - i\omega} + \frac{B}{1 - i\omega} \\
A - i\omega A + B\omega_a - i\omega B &= 1 \\
A &= -B \\
A &= \frac{1}{1 - \omega_a}
\end{aligned} \tag{38}$$

and substituting equation (38) into (35) gives

$$p_2(Y) = \frac{1}{(1 - \omega_a)} \frac{1}{(1 + 2x_a)} (e^{-\omega_a Y} - e^{-Y}), \tag{39}$$

and the corresponding probability of detection is

$$\begin{aligned}
P_D &= \left(\frac{1}{2x_a} \right) \left[(1 + 2x_a) e^{\frac{Y_o}{1+2x_a}} - e^{-Y_o} \right] \\
&\cong \left(1 + \frac{1}{2x_a} \right) e^{\frac{Y_o}{1+2x_a}}
\end{aligned} \tag{40}$$

where the last line in equation (40) is valid for signal-to-noise ratios greater than 10 (10 dB). From the mathematical principle of induction it is readily demonstrated that for arbitrary N,

$$P_D = \left(1 + \frac{1}{Nx_a} \right)^{N-1} e^{\frac{Y_o}{1+Nx_a}}, \tag{41}$$

a very simple closed form result. The corresponding probability of false alarm is obtained from equation (41) by making the substitution $x_a = 0$, obtaining

$$P_{FA} = e^{-Y_o}. \tag{42}$$

Figure 4 shows a plot of P_D versus $x_a = \frac{\sigma_T^2}{\sigma_n^2}$ in dB for $N = 1, 10$.

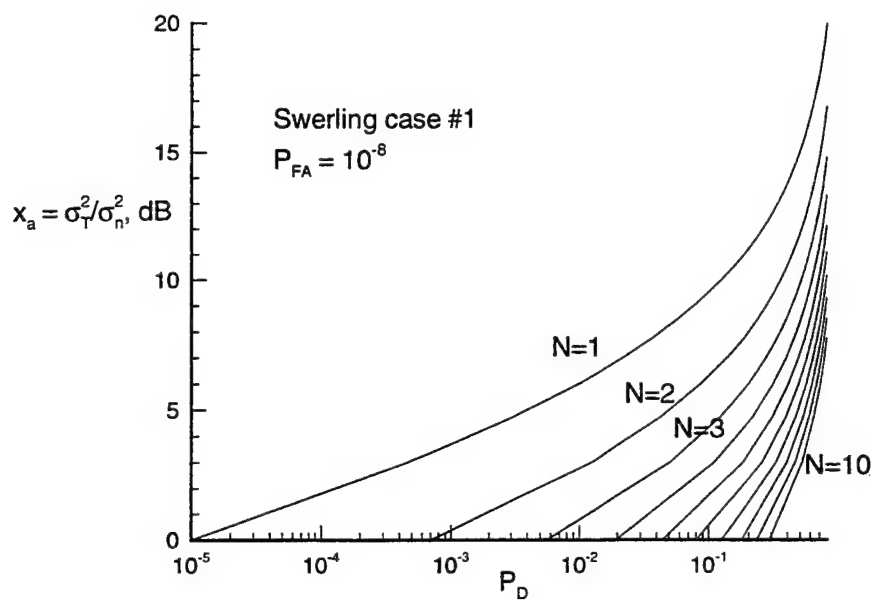


Fig. 4 Probability of Detection versus signal-to-noise ratio for a Swerling case #1 target, for $N=1, 10$.

2.4 Swerling Case #2:

From figure 2, we see the received signal is given by

$$Re^{i\theta} = \rho e^{i\psi} + re^{i\phi} . \quad (43)$$

where the first term on the right-hand-side of equation (43) fluctuates from pulse-to-pulse, and scan-to-scan. In this case the target is Rayleigh (the form given by Nathanson is exponential for the power which is Rayleigh for the voltage) and immersed in Rayleigh noise and the joint probability density of r and ϕ is given by

$$p_{r_n}(r, \phi) = \frac{r}{2\pi(\sigma_r^2 + \sigma_n^2)} e^{-\frac{r^2}{2(\sigma_r^2 + \sigma_n^2)}} , \quad (44)$$

where σ_r^2 is the target variance and σ_n^2 is the noise variance. Since we are again interested in obtaining the probability density of the square of the envelope in equation (43) it is convenient to define

$$\begin{aligned} y' &= \frac{R^2 / 2}{\sigma_r^2 + \sigma_n^2} = \frac{y}{1 + \frac{\sigma_r^2}{\sigma_n^2}} \\ y &= \frac{R^2 / 2}{\sigma_n^2} , \\ x' &= \frac{\rho^2 / 2}{\sigma_r^2 + \sigma_n^2} = \frac{x}{1 + \frac{\sigma_r^2}{\sigma_n^2}} = \frac{x}{1 + x_a} \end{aligned} \quad (45)$$

where equation (45) uses the same form for the definition of x' as in equation (7) for the normalized total power. The renormalization of x in (45) corresponds to a simple

substitution in all the derivations which follow. Equation (45) implies that the target variance plus noise variance are embedded (or included) in the pdf in equation (8) and do not need to be included again in the pdf for the target random variable, x . Thus the pdf is a delta function given by

$$p(x) = \delta(x). \quad (46)$$

The normalization in the first line in equation (45) is motivated by considering the total received power in each pulse. From equation (43), i.e.,

$$\begin{aligned} Re^{i\theta} &= \rho e^{i\psi} + r e^{i\phi} \\ |R|^2 &= |\rho e^{i\psi} + r e^{i\phi}|^2 \\ &= \rho^2 + r^2 + 2\rho r \cos(\psi - \phi) \\ \text{Exp}\{R^2\} &= \text{Exp}\{\rho^2\} + \text{Exp}\{r^2\} + 2\text{Exp}\{\rho r \cos(\psi - \phi)\} \\ \sigma_R^2 &= \sigma_r^2 + \sigma_n^2 \end{aligned} \quad (47)$$

For N-pulse detection of a Swerling case 2 target, where the target is varying from pulse-to-pulse, equation (13) is replaced by

$$Y' = y'_1 + y'_2 + \cdots + y'_N, \quad (48)$$

and, in the probability of detection Y_o is replaced with Y'_o . Substituting equation (46) into equation (13) yields the characteristic function for the SC-2 as

$$\begin{aligned} \Phi_N(\omega) &= \frac{1}{(1-i\omega)^N} \int_0^\infty e^{-Nx\left(1-\frac{1}{1-i\omega}\right)} \delta(x) dx \\ &= \frac{1}{(1-i\omega)^N} \end{aligned} \quad (49)$$

in agreement with DiFranco and Rubin (Equation 11.3-17a, page 404). We will see shortly, that SC-2 and SC-4 differ only in $p(x)$. Substituting (49) into equation (14) gives the N-pulse probability for Swerling case #2 as

$$p_N(Y') = \frac{(Y')^{N-1} e^{-Y'}}{(N-1)!}, \quad (50)$$

in agreement with Fehlner (his equation 17, page 19).

The probability of detecting a Swerling-2 target in noise is the probability that

$$Y' \geq \frac{Y_o}{1 + \frac{\sigma_T^2}{\sigma_n^2}} = \frac{Y_o}{1 + x_a} \quad (51)$$

or

$$P_D = \int_{\frac{Y_o}{1 + \frac{\sigma_T^2}{\sigma_n^2}}}^{\infty} p_N(Y') dY'. \quad (52)$$

and substituting equation (50) into equation (52) gives the following probability of detecting a Swerling #2 target as

$$P_D = e^{-\frac{Y_o}{1 + \frac{\sigma_T^2}{\sigma_n^2}}} \sum_{m=0}^{N-1} \left(\frac{Y_o}{1 + \frac{\sigma_T^2}{\sigma_n^2}} \right)^m \frac{1}{m!}, \quad (53)$$

another closed form result. The probability of false alarm is $P_{FA} = e^{-Y_o}$.

Figure 5 shows a plot of $x_a = \frac{\sigma_T^2}{\sigma_n^2}$ versus P_D for $P_{FA} = 10^{-8}$ for $N = 1, 2$

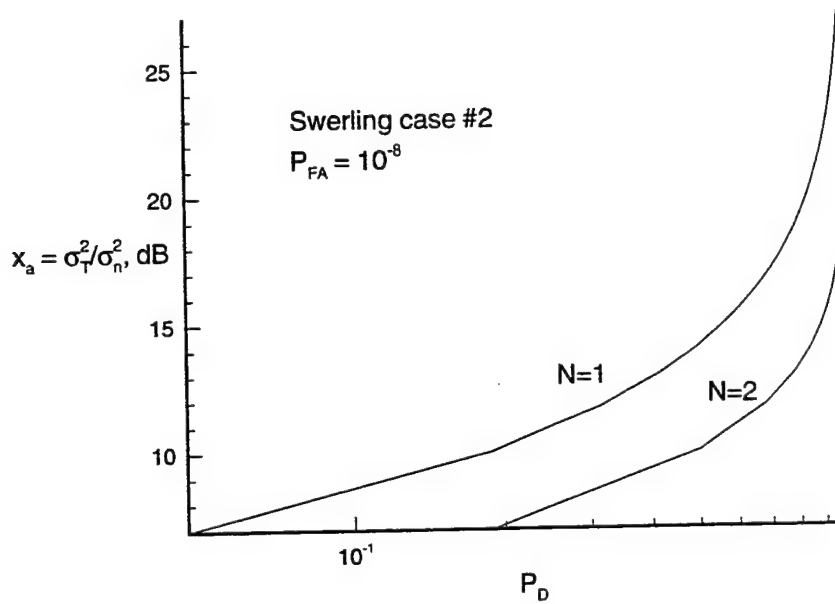


Fig. 5 Probability of detection versus signal-to-noise ratio for Swerling case #2 target with $N=1, 2$.

2.5 Swerling Case #3:

We see from figure 2, that the probability density function when one large scatterer exists with a number of small scatterers is, (Nathanson, page 86)

$$p(x) = \frac{x}{(x_a/2)^2} e^{-\frac{x}{x_a/2}}$$

$$x_a = \frac{\sigma_T^2}{\sigma_n^2}, \quad (54)$$

Substituting the last line of equation (54) into equation (13) gives

$$\begin{aligned} \Phi_N(\omega) &= \frac{4}{x_a^2 (1-i\omega)^N} \int_0^\infty e^{-\left(\frac{2}{x_a} \frac{i\omega N}{1-i\omega}\right)} x dx \\ &= \frac{\frac{4}{x_a^2}}{(1-i\omega)^N \left(\frac{2}{x_a} - \frac{i\omega N}{1-i\omega} \right)^2} \\ &= \frac{4}{(1-i\omega)^{N-2} [2 - i\omega(2 + Nx_a)]^2} \\ &= \frac{1}{(1-i\omega)^{N-2} \left[1 - i\omega \left(1 + \frac{Nx_a}{2} \right) \right]^2} \end{aligned} \quad (55)$$

which agrees with Fehner, page 26, his equation (A-8). Substituting equation (55) into equation (14) gives

$$p_N(Y) = \frac{1}{2\pi \left(1 + \frac{Nx_a}{2}\right)^2} \int_{-\infty}^{\infty} \frac{e^{-i\omega Y}}{(1-i\omega)^{N-2} (\omega_a - i\omega)^2} d\omega \quad (56)$$

$$\omega_a = \frac{1}{1 + \frac{Nx_a}{2}}$$

Again, we consider various cases for N starting with N=1:

$$\begin{aligned} p_1(Y) &= \frac{1}{2\pi \left(1 + \frac{x_a}{2}\right)^2} \int_{-\infty}^{\infty} \frac{(1-i\omega)e^{-i\omega Y}}{(\omega_a - i\omega)^2} d\omega \\ &= \frac{1}{2\pi \left(1 + \frac{x_a}{2}\right)^2} \left\{ \int_{-\infty}^{\infty} \frac{e^{-i\omega Y}}{(\omega_a - i\omega)^2} d\omega - i \int_{-\infty}^{\infty} \frac{\omega e^{-i\omega Y}}{(\omega_a - i\omega)^2} d\omega \right\} \\ &= \frac{1}{2\pi \left(1 + \frac{x_a}{2}\right)^2} \left[Y e^{-\omega_a Y} + Y e^{-\omega_a Y} \left(-\omega_a + \frac{1}{Y} \right) \right] \\ &= \frac{1}{2\pi \left(1 + \frac{x_a}{2}\right)^2} e^{-\omega_a Y} [1 + Y(1 - \omega_a)] \\ &= \frac{1}{2\pi \left(1 + \frac{x_a}{2}\right)^2} e^{-\omega_a Y} \left[1 + \frac{\left(\frac{x_a}{2}\right) Y}{1 + \frac{x_a}{2}} \right] \end{aligned} \quad (57)$$

and the corresponding probability of detection is

$$\begin{aligned}
P_D &= \int_{Y_o}^{\infty} p_1(Y) dY \\
&= \frac{1}{\left(1 + \frac{x_a}{2}\right)^2} \int_{Y_o}^{\infty} e^{-Y \left(\frac{1}{1 + \frac{x_a}{2}} \right)} \left[1 + \frac{Y \left(\frac{x_a}{2} \right)}{1 + \frac{x_a}{2}} \right] dY \\
&= e^{-\frac{Y_o}{1 + \frac{x_a}{2}}} \left\{ 1 + \frac{\frac{x_a}{2} Y_o}{\left(1 + \frac{x_a}{2}\right)^2} \right\}
\end{aligned} \tag{58}$$

An interesting observation for this particular case is that when $N = 1$, Fehner's derivation, (his equation A-3) yields infinity in the denominator, (unity divided by infinity equals zero), and this is the reason we suggest using equation (45). The mathematical result is correct, however, it is not convenient for numerical implementation.

The probability of false alarm for this case is

$$\begin{aligned}
P_{FA} &= \int_{Y_o}^{\infty} e^{-Y} Y dY \\
&= e^{-Y_o}
\end{aligned} \tag{59}$$

N=2:

$$\begin{aligned}
p_2(Y) &= \frac{1}{2\pi} \frac{1}{\left(1 + x_a\right)^2} \int_{-\infty}^{\infty} \frac{e^{-i\omega Y}}{(\omega_a - i\omega)^2} d\omega \\
&= \frac{Y e^{-\frac{Y}{1+x_a}}}{\left(1 + x_a\right)^2}
\end{aligned} \tag{60}$$

The probability of detection is

$$\begin{aligned}
P_D &= \int_{Y_o}^{\infty} p_2(Y) dY \\
&= e^{\frac{Y_o}{1+x_a}} \left[1 + \frac{Y_o}{1+x_a} \right],
\end{aligned} \tag{61}$$

and the corresponding probability of false alarm is

$$P_{FA} = e^{-Y_o} (1 + Y_o). \tag{62}$$

N=3:

$$\begin{aligned}
p_3(Y) &= \frac{1}{2\pi} \frac{1}{\left(1 + \frac{3x_a}{2}\right)^2} \int_{-\infty}^{\infty} \frac{e^{-i\omega Y}}{(1-i\omega)(\omega_a - i\omega)^2} d\omega \\
\frac{1}{(1-i\omega)(\omega_a - i\omega)^2} &= \frac{A}{1-i\omega} + \frac{B}{(\omega_a - i\omega)^2} + \frac{C}{\omega_a - i\omega} \\
1 &= A(\omega_a - i\omega)^2 + B(1-i\omega) + C(1-i\omega)(\omega_a - i\omega) \\
-\omega^2(A+C) &= 0 \\
-\omega(2i\omega_a A + iB + iC\omega_a + iC) &= 0 \\
A\omega_a^2 + B + C\omega_a &= 1 \\
A &= -C \\
A = \frac{1}{(\omega_a - 1)^2}, C = \frac{-1}{(\omega_a - 1)^2}, B = \frac{-1}{(\omega_a - 1)} & \tag{61}
\end{aligned}$$

and continuing,

$$p_3(Y) = \frac{1}{(3x_a/2)^2} e^{-Y} + \frac{Y e^{\frac{Y}{1+\frac{3x_a}{2}}}}{(3x_a/2) \left(1 + \frac{3x_a}{2}\right)} - \frac{1}{(3x_a/2)^2} e^{\frac{Y}{1+\frac{3x_a}{2}}} \quad (62)$$

The probability of detection becomes

$$P_D = \frac{\left(e^{-Y_o} - e^{\frac{Y_o}{1+\frac{3x_a}{2}}} \right)}{\left(\frac{3x_a}{2} \right)^2} + \frac{Y_o e^{\frac{Y_o}{1+\frac{3x_a}{2}}}}{\left(\frac{3x_a}{2} \right)} + \frac{\left(1 + \frac{3x_a}{2} \right)}{\frac{3x_a}{2}} e^{\frac{Y_o}{1+\frac{3x_a}{2}}} \quad (63)$$

and the probability of false alarm is

$$P_{FA} = (1 + Y_o) e^{-Y_o} \quad (64)$$

The analysis required to solve for Y_o for $N=2$, is as follows:

$$\begin{aligned}
\log_e P_{FA} &= \log_e (1 + Y_o) - Y_o \\
&\cong \frac{Y_o}{1 + \frac{Y_o}{2 + \frac{Y_o}{3 + \frac{Y_o}{4 + \dots}}}} - Y_o \\
Y_o^2 + \log_e P_{FA} Y_o + 2 \log_e P_{FA} &= 0 \\
Y_o &= -\frac{1}{2} \log_e P_{FA} + \sqrt{\frac{1}{4} (\log_e P_{FA})^2 - 2 \log_e P_{FA}}
\end{aligned}$$

Figure 6 shows a plot of $x_a = \frac{\sigma_T^2}{\sigma_n^2}$ versus P_D for $P_{FA} = 10^{-8}$, for $N = 1, 2$ and 3 . In order to be able to compare our results with DiFranco and Rubin, their definition for normalized signal-to-noise power has to be related to our definition in equation (7). DiFranco and Rubin define

$$x_{D-R} = 3 \frac{\rho^2 / 2}{\sigma_n^2}.$$

This results in the mean signal power power as

$$\begin{aligned}
A^2 &= \text{Exp}\{x_{D-R}^2\} = \frac{4}{3} A_o^2 \\
x^2 &= \frac{\rho^2 / 2}{\sigma_n^2} = \frac{A^2}{2 A_o^2}
\end{aligned}$$

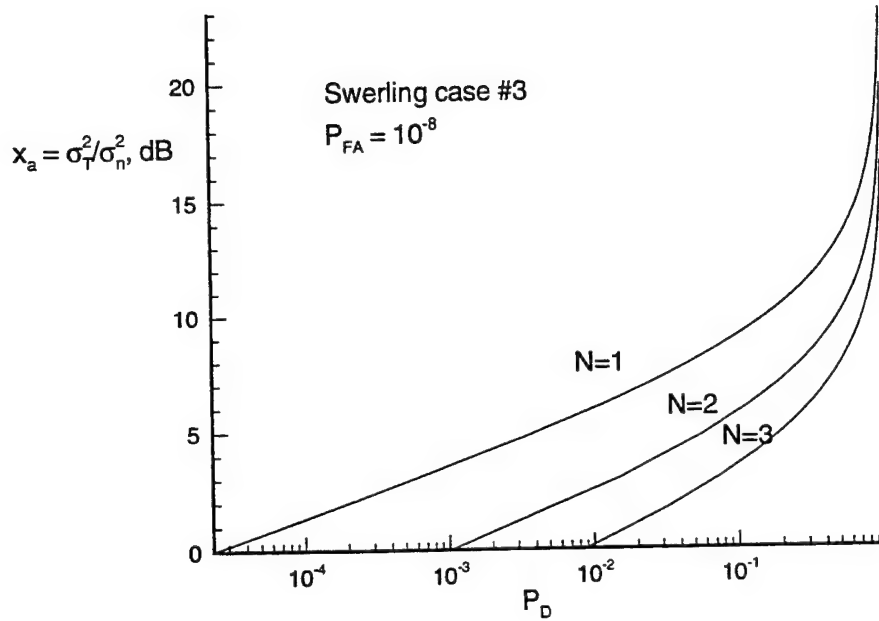


Fig. 6 Probability of detection versus signal-to-noise ratio for Swerling #3 target.

For example, from figure 6

$$P_D = 0.1, N = 1, x_a = 9.0 \text{ dB}.$$

From figure 11.4-1, page 411 of DiFranco and Rubin at

$$P_D = 0.1 (10\%), \overline{\mathfrak{R}}_p = 12.2 - 3.0 = 9.2 \text{ dB},$$

where we need to subtract 3 dB because DiFranco and Rubin use peak power and we use average power. The above results are within numerical accuracy in reading their plot. From Fehlnert, page 67, figure 31, for $P_D = 0.1, S/N = 8.0 (9.0 \text{ dB})$. For $N = 2, P_D = 0.1$, from figure 6, $S/N = 6.5 \text{ dB}$, and from Fehlnert, figure 32, page, $N = 2, P_D = 0.1, S/N = 6.53 \text{ dB}$, which is excellent agreement.

2.6 Swerling Case #4:

As discussed in section 1.1, the order of applying the pdf for the target power, and treating the sum of N-pulses needs to be interchanged from the previous Swerling cases. To evaluate the characteristic function for SC-4, we average with respect to $p(x)$. For SC-4, $p(x)$ is the pdf for one dominant scatterer plus noise. For SC-2, $p(x)$ is the pdf for all the returns in figure 2. For SC-4, we first average over $p(x)$ and then address the N-pulse case. Using the same pdf for the target as in SC-3 (Nathanson), we have from the last line in equation (9),

$$\begin{aligned}
 \Phi(\omega) &= \int_0^{\infty} \Phi(\omega|x) p(x) dx \\
 &= \frac{1}{(1-i\omega)} \int_0^{\infty} \frac{x}{\left(\frac{x_a}{2}\right)^2} e^{-\frac{x}{x_a/2}} e^{\frac{i\omega x}{1-i\omega}} dx \\
 &= \frac{(1-i\omega)}{\left(1+\frac{x_a}{2}\right)^2 \left[\frac{1}{1+\frac{x_a}{2}} - i\omega \right]^2} , \tag{65}
 \end{aligned}$$

Substituting equation (65) into equation (14) ($\Phi_N(\omega) = [\Phi(\omega)]^N$) gives for the N-pulse case

$$p_N(Y) = \frac{1}{2\pi} \frac{1}{\left(1+\frac{x_a}{2}\right)^{2N}} \int_{-\infty}^{\infty} \frac{(1-i\omega)^N e^{-i\omega Y}}{\left[\frac{1}{1+\frac{x_a}{2}} - i\omega \right]^{2N}} d\omega , \tag{66}$$

where the integrand of equation (66) agrees with Fehlner (1962, page 426, equation A-13).

We again consider cases beginning with N=1:

$$\begin{aligned}
 p_1(Y) &= \frac{1}{2\pi} \frac{1}{\left(1 + \frac{x_a}{2}\right)^2} \int_{-\infty}^{\infty} \frac{(1 - i\omega)}{\left(\frac{1}{1 + \frac{x_a}{2}} - i\omega\right)^2} e^{-i\omega Y} d\omega \\
 &= \omega_a^2 e^{-\omega_a Y} \left[1 + \omega_a \left(\frac{x_a}{2}\right) Y \right]
 \end{aligned} \tag{67}$$

which agrees with SC-3 for N=1. The corresponding probability of detection is

$$\begin{aligned}
 P_D &= \int_{Y_o}^{\infty} p_1(Y) dY \\
 &= e^{-\omega_a Y_o} \left[1 + \omega_a^2 \left(\frac{x_a}{2}\right) Y_o \right] \\
 \omega_a &= \frac{1}{1 + \frac{x_a}{2}}
 \end{aligned} \tag{68}$$

The probability of false alarm is

$$P_{FA} = e^{-Y_o} \tag{69}$$

N=2:

$$\begin{aligned}
p_2(Y) &= \frac{1}{2\pi} \frac{1}{\left(1 + \frac{x_a}{2}\right)^4} \int_{-\infty}^{\infty} \frac{(1 - i\omega)^2 e^{-i\omega Y}}{\left(\frac{1}{1 + \frac{x_a}{2}} - i\omega\right)^4} d\omega \\
&= \frac{1}{2\pi} \frac{1}{\left(1 + \frac{x_a}{2}\right)^4} \int_{-\infty}^{\infty} \frac{(1 - 2i\omega - \omega^2)}{\left(\frac{1}{1 + \frac{x_a}{2}} - i\omega\right)^4} e^{-i\omega Y} d\omega \\
&= \omega_a^4 Y^3 e^{-\omega_a Y} \left(\frac{\omega_a^2 x_a^2}{6} + \frac{x_a \omega_a}{Y} + \frac{1}{Y^2} \right) \\
\omega_a &= \frac{1}{1 + \frac{x_a}{2}} \tag{70}
\end{aligned}$$

The probability of detection is

$$P_D = \omega_a^2 e^{-\omega_a Y_o} \left[\begin{aligned} &\left(1 + \frac{x_a}{2}\right)^2 + \omega_a Y_o \left(1 + \frac{x_a}{2}\right)^2 \\ &+ \frac{x_a}{2} (\omega_a Y_o)^2 \left(1 + \frac{x_a}{4}\right) + \\ &\frac{\left(\frac{x_a}{2}\right)^2 (\omega_a Y_o)^3}{6} \end{aligned} \right], \tag{71}$$

and the probability of false alarm is

$$P_{FA} = e^{-Y_o} (1 + Y_o). \quad (72)$$

N=3:

$$p_3(Y) = \frac{1}{2\pi} \frac{1}{\left(1 + \frac{x_a}{2}\right)^6} \int_{-\infty}^{\infty} \frac{(1 - i\omega)^3 e^{-i\omega Y}}{\left(\frac{1}{1 + \frac{x_a}{2}} - i\omega\right)^6} d\omega$$

$$\frac{Y^5 e^{-\omega_a Y}}{\Gamma(6) \left(1 + \frac{x_a}{2}\right)^6} \left[1 + \left(-\omega_a + \frac{5}{Y}\right) + \left(\omega_a^2 - \frac{10\omega_a}{Y} + \frac{20}{Y^2}\right) + \left(-\omega_a^3 + \frac{15\omega_a^2}{Y} - \frac{60\omega_a}{Y^2} + \frac{60}{Y^3}\right) \right] \quad (73)$$

The probability of detection is

$$P_D = \frac{\left(\frac{x_a}{2}\right) \omega_a^6 e^{-\omega_a Y_o}}{\Gamma(6)} \left[\frac{Y_o^5 (1 - 2\omega_a + \omega_a^2) + \frac{5}{\omega_a} Y_o^4 (1 + \omega_a - 2\omega_a^2) + \frac{20}{\omega_a^2} (1 + \omega_a + \omega_a^2)}{\left(Y_o^3 + \frac{3}{\omega_a} Y_o^2 + \frac{6}{\omega_a^2} Y_o + \frac{6}{\omega_a^3}\right)} \right] \quad (74)$$

The probability of false alarm is

$$P_{FA} = e^{-Y_o} \left(1 + Y_o + \frac{Y_o^2}{2} \right) \quad (75)$$

Figure 7 shows a plot of $x_a = \frac{\sigma_T^2}{\sigma_n^2}$ versus P_D for $N = 1, 2, 3$.

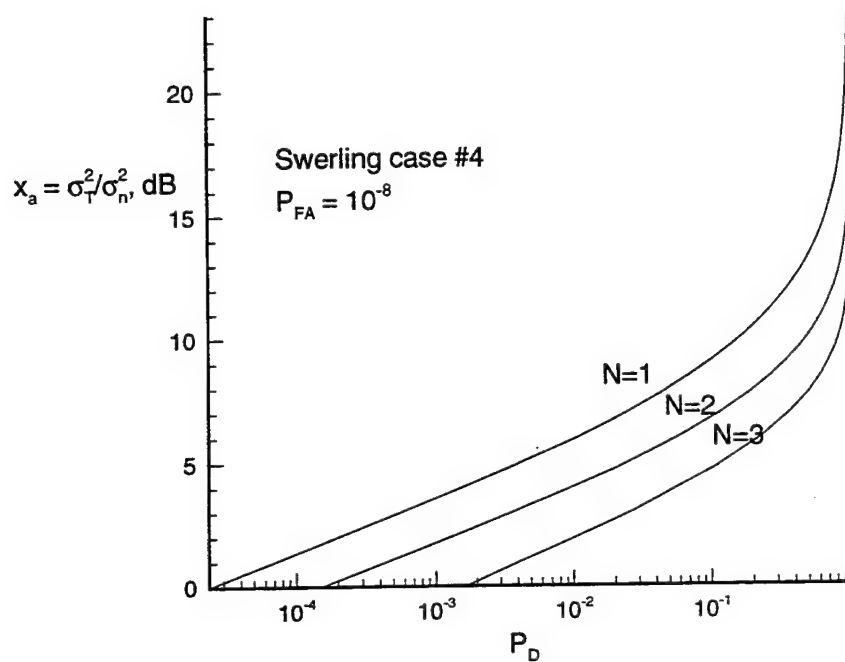


Fig. 7 Probability of detection versus signal-to-noise ratio for Swerling case #4 target.

2.7 Swerling Target plus Compound-k Clutter and Gaussian Noise

The probability density function for the sum of the target plus clutter signal in equation (3) is

$$\rho e^{i\psi} = \tau e^{i\omega} + \gamma e^{i\zeta} . \quad (76)$$

For a Rayleigh target, with uniformly distributed phase, ω , we know that

$$p_{\tau}(\tau, \omega) = \frac{\tau}{2\pi\sigma_{\tau}^2} e^{-\frac{\tau^2}{2\sigma_{\tau}^2}} , \quad (77)$$

and the pdf for the sum in equation (76) of two Rayleigh phasors (i.e., γ is also Rayleigh distributed) is (Beckmann, page 124, equation 4.5-4)

$$p_{\tau_c}(\rho) = \frac{\rho}{\sigma_{\tau}^2} e^{-\frac{\rho^2}{2\sigma_{\tau}^2}} \int_0^{\infty} p_c(\gamma) e^{-\frac{\gamma^2}{2\sigma_{\tau}^2}} I_0\left(\frac{\rho\gamma}{\sigma_{\tau}^2}\right) d\gamma . \quad (78)$$

In section 4, we show that when a Rayleigh pdf representing “spikey” clutter, with clutter variance, σ_c^2 , is modulated by a gamma pdf, the resulting pdf is the so-called compound-K clutter pdf. The principal features of a high-resolution radar return from the sea consist of a fast time variation within a resolution cell (the so-called temporal variation on time scales on the order of several millisecond) and a slow time variation from cell to cell (the so-called spatical variation on time scales on the order of several seconds). We assume the sea is frozen on a pulse-to-pulse basis (this would be valid for pulse repetition intervals of 10 millisecond based on the decorrelation time for sea scatter). The fast time features of the return are “spikey” and have a Rayleigh pdf. The reason the short time statistics are Rayleigh, is the surface slopes on the sea follow a Gaussian pdf, and the resulting scattered field is Gaussing in the I and Q components, or a Rayleigh envelope. The slow time variation, or the envelope of the return is modulated by the gamma pdf, because the swell moves in and out of a particular slant range cell. As shown in section 4, when the compound-K statistics are included, we will require the clutter variance in the Rayleigh pdf to satisfy

$$\sigma_c^2 = \frac{\kappa^4 + 3\kappa^3 - 2\kappa + 1}{(\alpha\kappa)^2}, \quad (79)$$

where α defines the mean value of the clutter power and κ defines a shape parameter that defines the clutter variance. In order to proceed, we assume in (78) that

$$p_c(\gamma|\sigma_c^2) = \frac{\gamma}{\sigma_c^2} e^{-\frac{\gamma^2}{2\sigma_c^2}}, \quad (80)$$

where the pdf for the clutter amplitude is conditioned on the clutter variance as shown in section 4. As will be seen in section 4, this conditional form for the pdf introduces mathematical complications which do not permit writing the probability of detection in closed form, and to proceed, we take the approach that the clutter variance in (80) be treated as simply an ordinary probability assuming σ_c^2 is a variable. Substituting (80) into (78) yields

$$\begin{aligned} p_{\tau_c}(\rho) &= \frac{\rho}{\sigma_r^2 \sigma_c^2} e^{-\frac{\rho^2}{2\sigma_r^2}} \int_0^\infty e^{-\frac{\gamma^2}{2} \left(\frac{1}{\sigma_r^2} + \frac{1}{\sigma_c^2} \right)} I_0 \left(\frac{\rho\gamma}{\sigma_r^2} \right) \gamma d\gamma \\ &= \frac{\rho}{\sigma_r^2 \sigma_c^2} e^{-\frac{\rho^2}{2\sigma_r^2}} \frac{\sigma_r^2 \sigma_c^2}{(\sigma_r^2 + \sigma_c^2)} e^{-\frac{\rho^2}{2\sigma_r^2} \frac{\sigma_r^2 \sigma_c^2}{(\sigma_r^2 + \sigma_c^2)}} \\ &= \frac{\rho}{(\sigma_r^2 + \sigma_c^2)} e^{-\frac{\rho^2}{2(\sigma_r^2 + \sigma_c^2)}} \end{aligned} \quad (81)$$

Recall that $x = \frac{\rho^2 / 2}{\sigma_n^2}$, and it is easy to show that

$$p_{\tau_c}(x) = \frac{1}{\left(\frac{\sigma_r^2}{\sigma_n^2} + \frac{\sigma_c^2}{\sigma_n^2} \right)} e^{-\frac{x}{\left(\frac{\sigma_r^2}{\sigma_n^2} + \frac{\sigma_c^2}{\sigma_n^2} \right)}}. \quad (82)$$

We now substitute (82) in (13) to obtain

$$\Phi_N(\omega) = \frac{\omega_c}{(1-i\omega)^{N-1}(\omega_c-i\omega)}$$

$$\omega_c = \frac{1}{1+N\left(\frac{\sigma_T^2}{\sigma_n^2} + \frac{\sigma_c^2}{\sigma_n^2}\right)} \quad (83)$$

Now substitute (83) into (14) to find

$$p_N(Y) = \frac{\omega_c}{2\pi} \int_{-\infty}^{\infty} \frac{e^{-i\omega Y}}{(1-i\omega)^{N-1}(\omega_c-i\omega)} d\omega. \quad (84)$$

where, in several steps above we have made use of the following result

$$F(a,b) = \int_0^{\infty} e^{-a^2 x^2} I_0(bx) x dx$$

$$I_0(bx) = \sum_{k=0}^{\infty} \frac{\left(\frac{b^2 x^2}{4}\right)^k}{k! \Gamma(k+1)}$$

$$\int_0^{\infty} e^{-a^2 x^2} x^{2k+1} dx = \frac{1}{2a^{2k+2}} \Gamma(K+1). \quad (85)$$

$$F(a,b) = \frac{1}{2a^2} \sum_{k=0}^{\infty} \left(\frac{b^2}{4a^2}\right)^k \frac{1}{k!}$$

$$= \frac{1}{2a^2} e^{\frac{b^2}{4a^2}}$$

We now examine specific values for N.

N=1:

$$p_1(Y) = \omega_c e^{-\omega_c Y}, \quad (86)$$

and the probability of detection is

$$P_D = e^{-\omega_c Y_o} \quad (87)$$

The corresponding probability of false alarm is

$$\begin{aligned} P_{FA} &= e^{-\omega_c^o Y_o} \\ \omega_c^o &= 1 + N \left(\frac{\sigma_c^2}{\sigma_n^2} \right) \\ y_o &= - \left[1 + N \left(\frac{\sigma_c^2}{\sigma_n^2} \right) \right] \ln(P_{FA}) \end{aligned} \quad (88)$$

N=2:

$$\Phi_2(\omega) = \frac{\omega_c}{(1 - \omega_c)} \left(\frac{1}{\omega_c - i\omega} - \frac{1}{1 - i\omega} \right). \quad (89)$$

and substituting (89) into (14) gives

$$p_2(Y) = \frac{\omega_c}{1 - \omega_c} (e^{-\omega_c Y} - e^{-Y}), \quad (90)$$

and the probability of detection is

$$P_D = \frac{\omega_c}{(1 - \omega_c)} \left(\frac{1}{\omega_c} e^{-\omega_c Y_o} - e^{-Y_o} \right), \quad (91)$$

and the probability of false alarm is given in (88).

N=3:

$$p_3(Y) = \frac{\omega_c}{(1 - \omega_c)^2} (-e^{-Y} + Y e^{-Y} + e^{-\omega_c Y}) \quad (92)$$

The probability of detection is

$$P_D = \frac{1}{(1 - \omega_c)^2} e^{-\omega_c Y}, \quad (93)$$

and the probability of false alarm is given in (88).

In general, from induction, the probability of detection for this case for any N is

$$P_D(N) \cong \frac{1}{(1 - \omega_c)^{N-1}} e^{-\omega_c Y_o} \quad (94)$$

Figure 8 shows a plot of $\frac{\sigma_r^2}{\sigma_n^2}$ in dB versus P_D for a target-to-clutter ratio,

$$\frac{\sigma_r^2}{\sigma_c^2} = 1 \text{ (a "stressing" case), for } N=1, 2 \text{ and } 3.$$

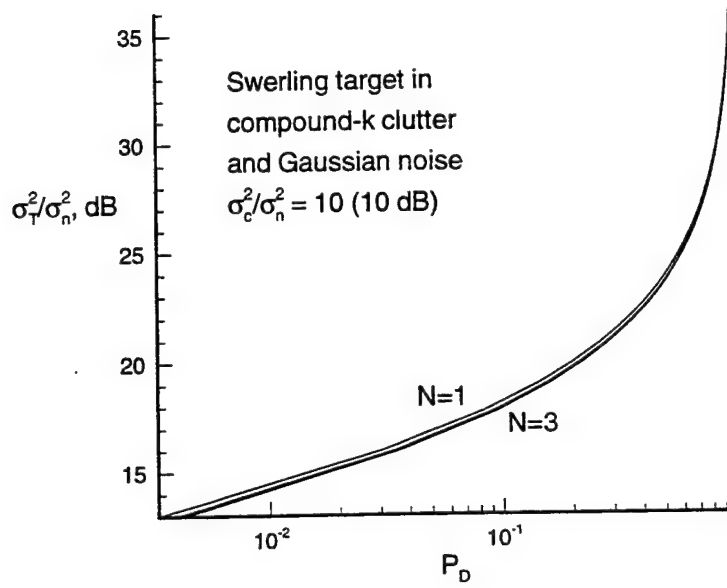


Fig. 8 Probability of detection versus signal-to-noise ratio for a target in clutter plus noise. Three different cases for the number of integrated pulses are considered.

From figure 8 we see for the case examined, where the target-to-clutter ratio is 10 (a stressing case), there is relatively little significant improvement by integrating more pulses.

We now give an alternative derivation for probability of the sum in (76). The pdf for target plus noise can be written as

$$p(\rho|\gamma) = \frac{1}{2\pi\sigma_r^2} e^{-\frac{(x-\tau)^2 + y^2}{2\sigma_r^2}}, \quad (95)$$

and we wish to determine the pdf of

$$\begin{aligned}
\rho &= \sqrt{x^2 + y^2} \\
x &= \tau e^{i\omega} \\
y &= \gamma e^{i\zeta}
\end{aligned} \tag{96}$$

We make the transformation of variables

$$x = \rho \cos \theta, y = \rho \sin \theta, dx dy = \rho d\rho d\theta \tag{97}$$

to obtain

$$\begin{aligned}
p(\rho|\tau) &= \frac{1}{2\pi\sigma_T^2} \int_0^{2\pi} e^{-\frac{(\rho \cos \theta - \tau)^2 + (\rho \sin \theta)^2}{2\sigma_T^2}} \rho d\rho d\theta \\
&= \frac{\rho}{2\pi\sigma_T^2} e^{-\frac{(\rho^2 + \tau^2)}{2\sigma_T^2}} \int_0^{2\pi} e^{\rho \cos \theta / \sigma_T^2} d\theta \\
&= \frac{\rho}{\sigma_T^2} e^{-\frac{(\rho^2 + \tau^2)}{2\sigma_T^2}} I_0\left(\frac{\rho\tau}{\sigma_T^2}\right)
\end{aligned} \tag{98}$$

Again, using the variable $x = \frac{\rho^2}{2\sigma_n^2}$, equation (98) becomes

$$p(x|\gamma) = \left(\frac{\sigma_n^2}{\sigma_T^2}\right) e^{-\left(\frac{\sigma_n^2}{\sigma_T^2}x + \frac{\tau^2}{2\sigma_T^2}\right)} I_0\left(\frac{\gamma\sqrt{2x\sigma_n^2}}{\sigma_T^2}\right). \tag{99}$$

Then from the Theorem of Total Probability

$$\begin{aligned}
p(x) &= \int_0^\infty p(x|\gamma) p(\gamma) d\gamma \\
p(x) &= \left(\frac{\sigma_n^2}{\sigma_T^2} \right) \int_0^\infty e^{-\left[\left(\frac{\sigma_n^2}{\sigma_T^2} \right) x + \frac{\gamma^2}{2\sigma_T^2} \right]} I_0 \left(\frac{\gamma \sqrt{2x\sigma_n}}{\sigma_T^2} \right) p(\gamma) d\gamma \\
&= \left(\frac{\sigma_n^2}{\sigma_T^2} \right) \left(\frac{1}{\sigma_c^2} \right) e^{-\frac{\sigma_n^2}{\sigma_T^2} x} \int_0^\infty e^{-\frac{\gamma^2}{2(\sigma_T^2 + \sigma_c^2)}} I_0 \left(\frac{\gamma \sqrt{2x\sigma_n}}{\sigma_T^2} \right) \gamma d\gamma, \quad (100) \\
&= \left(\frac{\sigma_n^2}{\sigma_T^2} + \frac{\sigma_n^2}{\sigma_c^2} \right) e^{-\frac{x}{\left(\frac{\sigma_n^2}{\sigma_T^2} \right) \left(\frac{\sigma_n^2}{\sigma_c^2} \right)}}
\end{aligned}$$

in agreement with equation (81).

3. An Alternative Derivation for the Probability Density Function for a Target and Gaussian Noise Fluctuating Pulse-to-Pulse (Swerling Class 2, N=1).

As an alternative to the derivation in section 1.2, consider the following analysis. When the target varies so rapidly that its cross section changes from pulse-to-pulse along with the noise, we can replace equation (1) for the total received signal in the I and Q channels (no clutter) as

$$Re^{i\theta} = \tau e^{i\omega} + re^{i\phi}, \quad (101)$$

and the probability density function for the received signal in equation (101) is, assuming the target is Rayleigh distributed, and the noise is a uniformly distributed phasor (with random amplitude),

$$\begin{aligned} p(R|r) &= \frac{R}{\sigma_T^2} e^{-\frac{(R^2+r^2)}{2\sigma_T^2}} I_0\left(\frac{Rr}{\sigma_T^2}\right) \\ y &= \frac{R^2}{2\sigma_T^2} \\ x &= \frac{r^2}{2\sigma_T^2} \\ p(y|x) &= e^{-(x+y)} I_0(2\sqrt{xy}), \quad y \geq 0 \end{aligned} \quad (102)$$

Then applying the Theorem of Total Probability,

$$p(y) = \int_{-\infty}^{\infty} p(y|x)p(x)dx, \quad (103)$$

and, assuming the noise in equation (103) is Rayleigh (Gaussian in I and Q and Rayleigh envelope)

$$p(x)dx = \frac{x}{\sigma_n^2} e^{-\frac{x^2}{2\sigma_n^2}} dx$$

$$y = \frac{\sigma_i^2 x^2}{2\sigma_n^4}, \left(\frac{\sigma_n^2}{\sigma_i^2} \right) dy = \frac{x dx}{\sigma_n^2}, \quad (104)$$

$$p(y)dy = \left(\frac{\sigma_n^2}{\sigma_i^2} \right) e^{-y \frac{\sigma_n^2}{\sigma_i^2}} dy$$

and substituting equation (104) into equation (103) gives $(x = \zeta^2, dz = 2\zeta d\zeta)$

$$p(y) = 2e^{-y} \frac{\sigma_n^2}{\sigma_T^2} \int_0^\infty e^{-\left(1 + \frac{\sigma_n^2}{\sigma_T^2}\right)\zeta^2} I_0(2\zeta\sqrt{y}) \zeta d\zeta$$

$$= \frac{\sigma_n^2}{\sigma_T^2} \frac{e^{-\frac{y \frac{\sigma_n^2}{\sigma_T^2}}{1 + \frac{\sigma_n^2}{\sigma_T^2}}}}{\left(1 + \frac{\sigma_n^2}{\sigma_T^2}\right)}, \quad (105)$$

$$= \frac{\sigma_n^2}{(\sigma_T^2 + \sigma_n^2)} e^{-y \frac{\sigma_n^2}{(\sigma_T^2 + \sigma_n^2)}}$$

a simple, closed form result.

An alternative derivation from Papoulis (pages 194-195, 1965) is as follows:

$$R^2 = \tau^2 + r^2$$

$$p(\tau, r) = \frac{1}{2\pi(\sigma_i^2 + \sigma_n^2)} e^{-\frac{(\tau^2 + r^2)}{2(\sigma_i^2 + \sigma_n^2)}}, \quad (106)$$

and assume the target has a mean value of

$$\text{Exp}\{\tau\} = \tau_1, \quad (107)$$

so the pdf in equation (106) becomes the Rice pdf as

$$\begin{aligned} p(z) &= \frac{1}{2\pi(\sigma_i^2 + \sigma_n^2)} \int_0^{2\pi} e^{\frac{(z \cos \vartheta - \tau_1)^2 + (z \sin \vartheta)^2}{2(\sigma_i^2 + \sigma_n^2)}} d\theta \\ &= \frac{z}{(\sigma_i^2 + \sigma_n^2)} e^{\frac{(z^2 + \tau_1^2)}{2(\sigma_i^2 + \sigma_n^2)}} I_0\left(\frac{z\tau_1}{\sigma_i^2 + \sigma_n^2}\right) \end{aligned} \quad (108)$$

We are again interested in obtaining the probability density of the square of the envelope of the total received signal. Thus define

$$\begin{aligned} \xi &= \frac{z^2}{2(\sigma_i^2 + \sigma_n^2)}, \quad \zeta = \frac{\tau_1^2}{2(\sigma_i^2 + \sigma_n^2)} \\ d\xi &= \frac{z dz}{(\sigma_i^2 + \sigma_n^2)}, \\ p(\xi|\zeta) &= e^{-(\xi+\zeta)} I_0(2\sqrt{\xi\zeta}) \end{aligned} \quad (109)$$

Now, we need to integrate the last line of equation (109) over all possible values of $\zeta(\tau_1)$ as

$$\begin{aligned} p(\xi) &= \int_0^\infty p(\xi|\zeta) d\zeta = e^{-\xi} \int_0^\infty e^{-\zeta} I_0(2\sqrt{\xi\zeta}) d\zeta \\ \zeta &= x^2, \quad d\zeta = 2x dx \\ p(\xi) &= 2e^{-\xi} \int_0^\infty e^{-x^2} I_0(2\sqrt{\xi}x) x dx = e^{-2\xi} = e^{-\frac{z^2}{(\sigma_i^2 + \sigma_n^2)}} \end{aligned} \quad (110)$$

which agrees with equation (104), with the following substitutions

$$\begin{aligned}
\xi &= \frac{y\sigma_n^2}{2(\sigma_T^2 + \sigma_n^2)}, z^2 = \frac{\sigma_n^2}{2\sigma_T^2} R^2, y\sigma_n^2 \\
p(z)dz &= p(\xi)d\xi \\
p(z) &= p(\xi) \frac{d\xi}{dz} = \frac{z}{(\sigma_n^2 + \sigma_T^2)} e^{-\frac{z^2}{2(\sigma_n^2 + \sigma_T^2)}}, \\
y &= \frac{z^2}{2}, dy = z dz
\end{aligned} \tag{111}$$

From equation (105) we can derive the probability of detection, P_D , and probability of false alarm, P_{FA} . We find

$$\begin{aligned}
P_D &= \int_{y_0}^{\infty} p(y) dy = e^{-\frac{y_0}{\left(1 + \frac{\sigma_T^2}{\sigma_n^2}\right)}} \\
P_{FA} &= \int_{y_0}^{\infty} e^{-y} dy = e^{-y_0} \\
y_0 &= -\log_e(P_{FA})
\end{aligned} \tag{112}$$

In figure 9 we plot the probability of detection for three false alarm numbers, or probability of false alarms determined from

$$P_{FA} = \frac{1}{n'} \log_e \left(\frac{1}{2} \right) = -\frac{0.693147}{n'}, \tag{113}$$

where n' is the false alarm number. The curves in figure 9 match those given by Fehlner (1962).

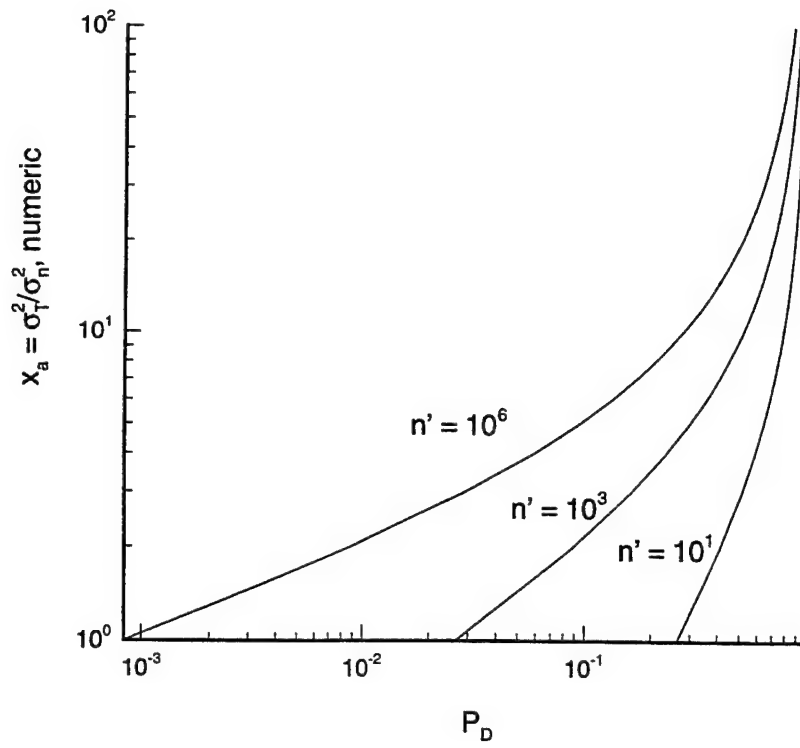


Fig. 9 Probability of detection of Swerling Class 2 targets in noise, for $N = 1$.

4. Probability Density Function for Broad-Band Clutter Constant Pulse-to-Pulse but Varying Scan-to-Scan (No Target, Probability of False Alarm)

From the free-space radar range equation, the received clutter-to-noise power is

$$\frac{P_c}{N} = \frac{P_r T_1 G^2 \lambda^2 \sigma_c}{(4\pi)^3 R^4 (k_o T_o)} |F|^4, \quad (114)$$

$$\sigma_c = (\phi_{3dB} R) \left(\frac{c T_1}{2} \right) \sigma_c^o$$

and the clutter variance, σ_c^2 , in the Rayleigh pdf,

$$p(\gamma|\sigma_c^2) = \frac{\gamma}{\sigma_c^2} e^{-\frac{\gamma}{\sigma_c^2}}. \quad (115)$$

is given by

$$\sigma_c^2 = \text{Exp}\{\sigma_c\} = (\phi_{3dB} R) \left(\frac{c T_1}{2} \right) \text{Exp}\{\sigma_c^o\}. \quad (116)$$

Ward et al.(1990) and Baker (1988), treat clutter by assuming the clutter is Rayleigh distributed on time scales of millsec as in equation (80), and assume the variance of the clutter in equation (115) is modulated with a Gamma probability density function, on time scales of seconds, as

$$p(\eta) = \frac{\alpha^{\kappa+1}}{\Gamma(\kappa+1)} \eta^{\kappa} e^{-\alpha\eta}. \quad (117)$$

where the random variable η (the clutter power) in equation (117) equals the clutter variance according to

$$\eta = 2\sigma_c^2, \quad (118)$$

and α is the mean value of the clutter power and K is a shape parameter that defines the normalized clutter variance.

The probability density function for the clutter amplitude, γ , is from the Theorem of Total Probability

$$\begin{aligned} p(\gamma) &= \int_0^{\infty} p_n(\gamma|\eta) p(\eta) d\eta \\ &= \frac{2\alpha^{K+1}\gamma}{\Gamma(K+1)} \int_0^{\infty} \eta^K e^{-\alpha\eta} \frac{1}{\eta} e^{-\frac{\gamma^2}{\eta}} d\eta \end{aligned} \quad (119)$$

The integral in equation (119) is evaluated as follows:

$$\begin{aligned} \alpha\eta + \frac{\gamma^2}{\eta} &= 2\sqrt{\alpha\gamma} \cosh \omega \\ \alpha\eta^2 - 2\eta\sqrt{\alpha\gamma} \cosh \omega + \gamma^2 &= 0 \\ \eta^2 - \frac{2\eta\gamma}{\sqrt{\alpha}} \cosh \omega + \frac{\gamma^2}{\alpha} &= 0 \\ \eta &= \frac{\gamma}{\sqrt{\alpha}} \cosh \omega \pm \sqrt{\frac{\gamma^2}{\alpha} \cosh^2 \omega - \frac{\gamma^2}{\alpha}} \\ &= \frac{\gamma}{\sqrt{\alpha}} (\cosh \omega \pm \sinh \omega) \\ \xrightarrow{\omega \rightarrow \infty} \eta &\rightarrow \infty, \quad \xrightarrow{\eta \rightarrow \infty} \omega \rightarrow \infty, (+) \\ \xrightarrow{\omega \rightarrow -\infty} \eta &\rightarrow 0, \quad \xrightarrow{\eta \rightarrow 0} \omega \rightarrow -\infty, (-) \\ d\eta &= \eta d\omega \\ \int_0^{\infty} \eta^K e^{-\alpha\eta} e^{-\frac{\gamma^2}{\eta}} \frac{d\eta}{\eta} &= \left(\frac{\gamma}{\sqrt{\alpha}} \right)^K \int_{-\infty}^{\infty} e^{-2\sqrt{\alpha\gamma} \cosh \omega} (\cosh \omega + \sinh \omega)^K d\omega \end{aligned} \quad (120)$$

The last integral is evaluated for the following cases:

$\kappa = 1$:

$$\begin{aligned} \frac{\gamma}{\sqrt{\alpha}} \int_{-\infty}^{\infty} e^{-2\sqrt{\alpha}\gamma \cosh \omega} (\cosh \omega + \sinh \omega) d\omega &= \frac{2x}{\sqrt{\alpha}} \int_0^{\infty} e^{-2\sqrt{\alpha}x \cosh \omega} \cosh \omega d\omega \\ &= \frac{2x}{\sqrt{\alpha}} K_1(2\sqrt{\alpha}x) \end{aligned}$$

$\kappa = 2$:

$$\begin{aligned} 2\left(\frac{\gamma}{\sqrt{\alpha}}\right)^2 \int_0^{\infty} e^{-2\sqrt{\alpha}x \cosh \omega} (\cosh \omega + \sinh \omega)^2 d\omega &= 2\left(\frac{x}{\sqrt{\alpha}}\right)^2 \int_0^{\infty} e^{-2\sqrt{\alpha}x \cosh \omega} (\cosh^2 \omega + \sinh^2 \omega) d\omega \\ &= 2\left(\frac{\gamma}{\sqrt{\alpha}}\right)^2 \int_0^{\infty} e^{-2\sqrt{\alpha}\gamma \cosh \omega} \cosh 2\omega d\omega \\ &= 2\left(\frac{\gamma}{\sqrt{\alpha}}\right)^2 K_2(2\sqrt{\alpha}\gamma) \end{aligned}$$

$\kappa = 3$:

$$\left(\frac{\gamma}{\sqrt{\alpha}}\right)^3 \int_{-\infty}^{\infty} e^{-2\sqrt{\alpha}\gamma \cosh \omega} (\cosh \omega + \sinh \omega)^3 d\omega = 2\left(\frac{\gamma}{\sqrt{\alpha}}\right)^3 K_3(2\sqrt{\alpha}\gamma)$$

(121)

and, in general,

$$\int_0^{\infty} \eta^{\kappa} e^{-\alpha\eta} e^{-\frac{\gamma^2}{\eta}} \frac{d\eta}{\eta} = 2\left(\frac{\gamma}{\sqrt{\alpha}}\right)^{\kappa} K_{\kappa}(2\sqrt{\alpha}\gamma), \quad (122)$$

and from (119) and (122),

$$\begin{aligned}
 p(\gamma) &= \frac{4\alpha^{\kappa+1}\gamma}{\Gamma(\kappa+1)} \left(\frac{\gamma}{\sqrt{\alpha}} \right)^{\kappa} K_{\kappa}(2\sqrt{\alpha}\gamma) \\
 &= \frac{4\alpha^{\frac{\kappa+1}{2}}\gamma^{\kappa+1}}{\Gamma(\kappa+1)} K_{\kappa}(2\sqrt{\alpha}\gamma)
 \end{aligned} \tag{120}$$

Figure 10 shows a plot of the pdf in equation (120) together with a Rayleigh pdf for comparison. If the form of the compound-K pdf given in equation (119) is substituted in the right-hand-side of equation (78) for $p_c(\gamma)$, the resulting integrand containing the product of two Bessel functions does not lend itself to a closed form representation. From figure 10, we see the tails of the compound-k distribution extend further out than the corresponding tails for the Rayleigh pdf. This probably accounts for the fact that the compound-k pdf predicts more “spikey” clutter than the Rayleigh pdf. This is also the reason in the design of a broad-band radar where the slant range cell is small, compared to that for a narrow band radar, that even though the slant range cell size is small, the clutter may appear more spikey than the corresponding return from a narrow band radar.

Figure 10 also shows the Rayleigh pdf over the same range of the independent variable. The mean value of the clutter parameter, α , is adjusted so that both pdf's have equal variances. We will see in equation (127) this is accomplished when $\kappa = 1$, if

$$\alpha = \frac{\sqrt{3}}{\sigma_c}.$$

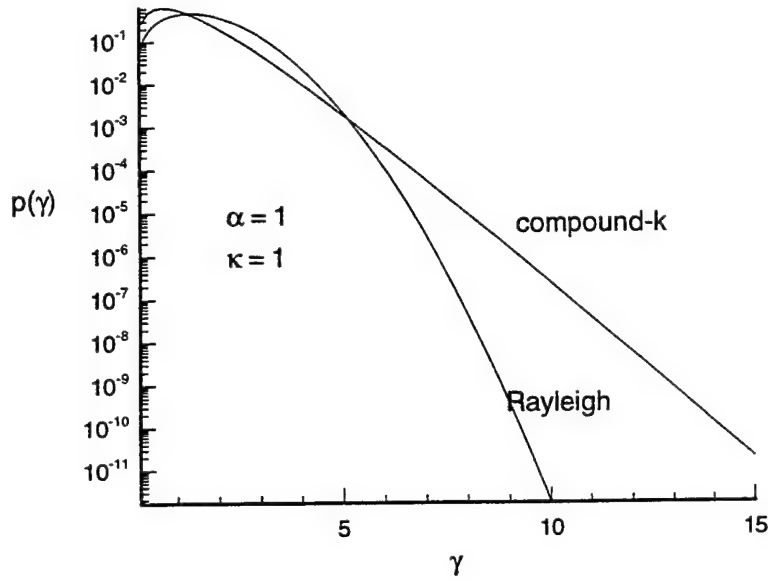


Fig. 10 A comparison of the compound-K and Rayleigh pdf's.

We now show a derivation for an approximate form for the compound-k pdf. Using the following asymptotic representation for the modified Bessel function in equation (123)

$$K_{\kappa}(z) \approx \sqrt{\frac{\pi}{2z}} e^{-z}, \quad (124)$$

equation (123) can be written as

$$p(\gamma) \cong \frac{2\sqrt{\pi}\alpha^{\frac{\kappa+1}{2}}\gamma^{\frac{\kappa+1}{2}}}{\Gamma(\kappa+1)} e^{-2\sqrt{\alpha}\gamma}, \quad (125)$$

and making the replacement in (125)

$$\kappa + \frac{1}{2} = \nu, \quad (126)$$

gives a form for $p(\gamma)$ identical to the gamma pdf (Papoulis, 1965, p. 103-104) as

$$p(\gamma) \equiv \frac{2\sqrt{\pi}}{\Gamma\left(\nu + \frac{1}{2}\right)} (\sqrt{\alpha})^{\nu+\frac{1}{2}} \gamma^{\nu} e^{-2\sqrt{\alpha}\gamma}, \quad (127)$$

with

$$\Gamma\left(\frac{1}{2}\right) = \sqrt{\pi}. \quad (128)$$

Thus, the probability density function for the clutter voltage (no target) can be approximated as

$$p(\gamma) \equiv \frac{\alpha^{\kappa+1}}{\Gamma(\kappa+1)} \gamma^{\kappa} e^{-\alpha\gamma}, \quad (129)$$

and we are back to a simple gamma pdf. The pdf in equation (129) represents a much simpler expression for use in integrals involving the Theorem of Total Probability. In figure 11, we show a plot of the approximate compound-k (gamma) pdf together with the exact pdf.

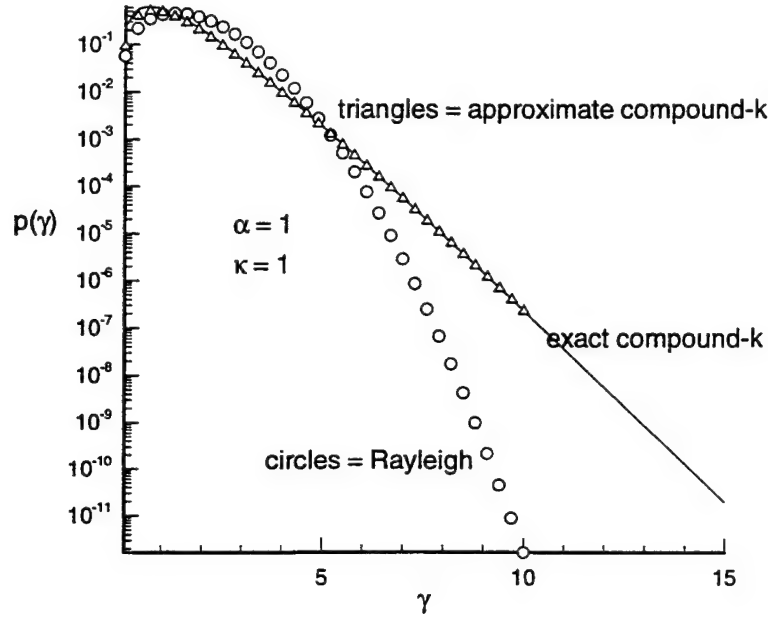


Fig. 11 Comparison of the approximate compound-k (equation 125) and the exact compound-k pdf (equation 119).

We have shown in figure 11 that using the approximate form for the compound-k pdf differs insignificantly from the exact expression, and therefore this simpler form should be considered in derivations requiring the compound-k pdf.

The first two moments of η are given by

$$\begin{aligned}
 \text{Exp}\{\gamma\} &= \bar{\gamma} = \frac{1}{\kappa\alpha} \\
 \text{Exp}\left\{\left(\gamma - \bar{\gamma}\right)^2\right\} &= \sigma_{\gamma}^2 = \frac{\alpha^{\kappa+1}}{\Gamma(\kappa+1)} \int_0^{\infty} \left(\gamma - \frac{1}{\kappa\alpha}\right)^2 \gamma^{\kappa} e^{-\alpha\gamma} d\gamma, \quad (130) \\
 &= \frac{(\kappa^4 + 3\kappa^3 - 2\kappa + 1)}{(\kappa\alpha)^2}
 \end{aligned}$$

The clutter variance, from equation (130) is defined as

$$\sigma_c^2 \equiv \sigma_\gamma^2 = \frac{(\kappa^4 + 3\kappa^3 - 2\kappa + 1)}{(\alpha\kappa)^2}. \quad (131)$$

The clutter variance, σ_c^2 , has been estimated to be 0.7 for low-sea-state clutter, 1.1 for ground clutter and as high as 1.6 for high-sea-state clutter. Table 1 shows the corresponding values for α , in the compound-K pdf

Table 1. Clutter variance and mean clutter power for various environments.

environment	σ_c^2	α^2
low-sea-states	0.7	4.29
ground	1.1	2.73
high-sea-state	1.6	1.875

The moments for the gamma distribution can be expressed in terms of the characteristic function as (Papoulis, 1965)

$$m_i = \frac{1}{\Phi_c^i(\omega)} \frac{\partial^i \Phi_c^i}{\partial \omega}, \quad (132)$$

and, if the moments in equation (133) are normalized to the variance, Ward has shown that all moments greater than $i = 2$ are zero (Ward, 1990). This reduces to a Gaussian distribution using the Central Limit Theorem argument.

5. References

- Abramowitz, M. and I A. Stegun, Handbook of Mathematical Functions, National Bureau of Standards, U. S. Department of Commerce, Applied Mathematics Series 55, June, 1964.
- Baker, C. J., J. M. Pink, R. J. A. Tough, A Statistical Model for Radar Target Detection in Clutter, U. S. National radar Conference, 19888.
- Beckman, P., Probability in Communication Engineering, Harcourt, Brace and World, New York, 1967, chapter 4.
- Blake, L. V., Radar Range-Performance Analysis, Artech House, Inc. Norwood, Ma., 1986.
- DiFranco, J. V. and W. L. Rubin, Radar Detection, Artech House, Inc. Dedham, Ma., 1968.
- Fehlner, L. F., Target Detection by Pulsed Radar, The Johns Hopkins University, Applied Physics Lab., Silver Spring, MD., TG 451. July, 1962
- Hansen, J. P. and V. F. Cavaleri, High-Resolution Radar Sea Scatter, Experimental Observations and Discriminants, NRL Report 8557, March, 1982, Naval Research Lab., Washington, D.C.
- Marcum, J. and Swerling, P. Studies of target detection by pulsed radar, IRE Transactions on Information theory, IT-6:2, 1960.
- Nathanson, F., J. P. Reilly, M. N. Cohen, Radar Design Principles, McGraw-Hill, New York, 1991.
- Olver, F. W. J., Asymptotics and Special Functions, Academic Press, Inc., New York, 1974.
- Papoulis, A., Probability, Random Variables, and Stochastic Processes, McGraw-Hill, New York, 1965.
- Schleher, D. Radar detection in log-normal clutter, IEEE International Radar Conference, IEEE Press (Publication No. 75 CH0938-1 AES), New York, 1975.
- Skolnik, M. I., Introduction to Radar Systems, second edition, page 24, equation 2.24, McGraw-Hill, New York, 1980.
- Trunk, G. and S. George, Detection of targets in non-Gaussian sea clutter, IEEE Transactions of Aerospace and Electronic Systems, AES-6, pages 620-628, 1970.

Ward, K. D., C. J. Baker, and S. Watts, Maritime Surveillance Radar, Part 1: Radar and Scattering from the Ocean Surface, IEE Proc., Vol. 137, Part F. No. 2, April, 1990, pp. 51-62.

6. Computer Code

```
C
C  CALCULATE THE PROBABILITY OF DETECTION FOR SC-0
C
```

```
COMMON/SC0/B
OPEN(UNIT=10,FILE='C:\tecplot\sc01.dat')
OPEN(UNIT=11,FILE='C:\tecplot\sc02.dat')
Y0 = 8.*ALOG(10.)
DO 1 I=1,40
  FI = I
  B = FI
  Z = 2.*SQRT(B*Y0)
  CALL TRAP1(0.,Z,SUM,15)
  PD1 = 1. - EXP(-B)*SUM
  WRITE(10,*) PD1,10.*ALOG10(B)
  WRITE(*,*) PD1,B
1 CONTINUE
  A = 1.e-08
  Y0 = (-0.5*ALOG(A) +
x    SQRT(0.25*ALOG(A)**2 - 2.*ALOG(A)))
  DO 2 J=1,40
    FJ = J
    B = FJ
    Z2 = 2.*SQRT(B*Y0)
    CALL TRAP2(0.,Z2,SUM2,15)
    PD2 = 1. - EXP(-2.*B)*SUM2
    WRITE(11,*) PD2,10.*ALOG10(B)
    WRITE(*,*) PD2,B
2 CONTINUE
  STOP
  END
```

```
SUBROUTINE TRAP1(A,B,SUM,N)
EXTERNAL FSC0
NN = N + 1
SUM = 0.
FN = N
D = (B-A)/FN
X = A
DO 10 I=1,NN
  J= (I-1)*(NN-I)
  C = 1.
  IF(J) 15,5,6
5 C = 0.5
6 SUM = SUM + C*FSC0(X)
10 X = X + D
  SUM = SUM*D
  RETURN
15 WRITE(*,*) 'INCORRECT INDEX'
  STOP
  END
```

```

SUBROUTINE TRAP2(A,B,SUM,N)
EXTERNAL FSC02
NN = N + 1
SUM = 0.
FN = N
D = (B-A)/FN
X = A
DO 10 I=1,NN
J= (I-1)*(NN-I)
C = 1.
IF(J) 15,5,6
5 C = 0.5
6 SUM = SUM + C*FSC02(X)
10 X = X + D
SUM = SUM*D
RETURN
15 WRITE(*,*) 'INCORRECT INDEX'
STOP
END

```

```

C
C   A FUNCTION USED IN SC-0
C
FUNCTION FSC0(X)
EXTERNAL BESSIO
COMMON/SC0/B
FSC0 = BESSIO(X)*X*EXP(-X**2/(4.*B))
RETURN
END

```

```

C
C   A FUNCTION USED IN SC-0
C
FUNCTION FSC02(X)
EXTERNAL BESSI1
COMMON/SC0/B
FSC02 = BESSI1(SQRT(2.)*X)*(X**2/(4.*SQRT(2.)*B**2))*
x   EXP(-X**2/(4.*B))
RETURN
END

```

```

C
C   PROBABILITY OF DETECTION FOR SC-1
C
OPEN(UNIT=10,FILE='C:\tecplot\sc1.dat')
Y0 = 10.*ALOG(10)
DO 2 K=1,10
  N=K
  PWR = N - 1
  DO 1 I= 1,100
    XA = I*.2
    PD = ((1. + (1./(N*XA)))**PWR)*EXP(-Y0/(1. + N*XA))
    WRITE(*,*) PD,10.*ALOG10(XA)
    WRITE(10,*) PD,10.*ALOG10(XA)
  1 CONTINUE
2 CONTINUE
RETURN
END

```

```

C
C   PROBABILITY OF DETECTION FOR SC-2
C
EXTERNAL FACTRL
OPEN(UNIT=10,FILE='C:\tecplot\sc2.dat')
Y0 = 8.*ALOG(10)
DO 1 I=1,100
  XA = I*0.2
  PD = EXP(-Y0/(1. + XA))
  WRITE(*,*) PD,10.*ALOG10(XA)
  WRITE(10,*) PD,10.*ALOG10(XA)
1 CONTINUE
RETURN
END

```

```

C
C   PROBABILITY OF DETECTION FOR SC-3
C
EXTERNAL FACTRL
OPEN(UNIT=10,FILE='C:\tecplot\sc3.dat')
Y0 = 8.*ALOG(10.)
WRITE(*,*) Y0
DO 1 I=1,200
XA = I
OMEGA1 = 1./(1. + (XA/2.))
PD1 = EXP(-Y0*OMEGA1)*(1. + (XA/2.)*Y0*OMEGA1**2)
WRITE(10,*) PD1,10.*ALOG10(XA)
C   WRITE(*,*) PD1,10.*ALOG10(XA)
1 CONTINUE
A = 1.e-08
Y0 = (-0.5*ALOG(A) +
x   SQRT(0.25*ALOG(A)**2 - 2.*ALOG(A)))
WRITE(*,*) Y0
DO 2 I=1,200
XA = I
OMEGA2 = 1./(1. + XA)
PD2 = EXP(-Y0*OMEGA2)*(1. + Y0*OMEGA2)
WRITE(10,*) PD2,10.*ALOG10(XA)
C   WRITE(*,*) PD2,10.*ALOG10(XA)
2 CONTINUE
DO 3 I=1,200
XA = I
OMEGA3 = 1./(1. + (3.*XA/2.))
PD3 = EXP(-Y0*OMEGA3)*(1. + (1./(3.*XA/2.))*(1. + Y0))
WRITE(10,*) PD3,10.*ALOG10(XA)
C   WRITE(*,*) PD3,10.*ALOG10(XA)
3 CONTINUE
RETURN
END

```

```

C
C   PROBABILITY OF DETECTION FOR SC-4
C
OPEN(UNIT=10,FILE='C:\tecplot\sc4.dat')
Y0 = 8.*ALOG(10.)
WRITE(*,*) Y0
N = 1
DO 1 I=1,200
  XA = I
  OMEGA = 1./(1. + N*(XA/2.))
  PD1 = EXP(-Y0*OMEGA)*(1. + (XA/2.)*OMEGA**2*Y0)
  WRITE(10,*) PD1,10.*ALOG10(XA)
C   WRITE(*,*) PD1,10.*ALOG10(XA)
1 CONTINUE
  A = 1.e-08
  Y0 = (-0.5*ALOG(A) +
x   Sqrt(0.25*ALOG(A)**2 - 2.*ALOG(A)))
  WRITE(*,*) Y0
  DO 2 I=1,200
    XA = I
    OMEGA = 1./(1. + 0.5*XA)
    PD2 = OMEGA**2*EXP(-Y0*OMEGA)*((1. + 0.5*XA)**2 +
x   OMEGA*Y0*(1. + 0.5*XA)**2 +
x   0.5*XA*OMEGA**2*Y0**2*(1. + 0.25*XA) +
x   (1./6.)*(0.5*XA)**2*(Y0*OMEGA)**3)
    WRITE(10,*) PD2,10.*ALOG10(XA)
C   WRITE(*,*) PD2,10.*ALOG10(XA)
2 CONTINUE
  PFA = 1.e-08
  CALL NEWTON(PFA,Y0)
  WRITE(*,*) Y0
  DO 3 I=1,200
    XA = I
    OMEGA = 1./(1. + 0.5*XA)
    PD3 = (0.5*XA)*(OMEGA**6)*EXP(-Y0*OMEGA)/120.*
x   (Y0**5*(1. - 2.*OMEGA + OMEGA**2)
x   +(5./OMEGA)*Y0**4*(1. + OMEGA - 2.*OMEGA**2)
x   +(20./OMEGA**2)*(1. + OMEGA + OMEGA**2)*(
x   Y0**3 + (3./OMEGA)*Y0**2 + (6./OMEGA**2)*Y0 +
x   (6./OMEGA**3)))
    WRITE(10,*) PD3,10.*ALOG10(XA)
C   WRITE(*,*) PD3,10.*ALOG10(XA)
3 CONTINUE
  RETURN
END

```

```
C
C   FIND THE THRESHOLD USING NEWTON'S METHOD FOR SC4
C
SUBROUTINE NEWTON(PFA,Y0)
Y0I = -ALOG(PFA)
R1 = (1. + Y0I + 0.5*Y0I**2)
R2 = EXP(-Y0I)
R3 = 0.5*Y0I**2
Y0 = Y0I - (PFA/(R2*R3) - R1/R3)
RETURN
END
```

```

C
C   PROBABILITY OF DETECTION FOR SC-5
C
OPEN(UNIT=10,FILE='C:\tecplot\sc5.dat')
A = 10.e-08
N=1
XB = 10.
Y0 = -(1. + N*XB)*ALOG(A)
WRITE(*,*) Y0
DO 1 I=1,200
XA = 20.*I
OMEGAC1 = 1./(1. + (XB + XA))
PD1 = EXP(-OMEGAC1*Y0)
WRITE(10,*) PD1,10.*ALOG10(XA)
WRITE(*,*) PD1,10.*ALOG10(XA)
1 CONTINUE
N=2
Y0 = -(1. + N*XB)*ALOG(A)
DO 2 I=1,200
XA = 20.*I
OMEGAC2 = 1./(1. + 2.*(XB + XA))
PD2 = (1./(1. - OMEGAC2))*EXP(-OMEGAC2*Y0)
WRITE(10,*) PD2,10.*ALOG10(XA)
WRITE(*,*) PD2,10.*ALOG10(XA)
2 CONTINUE
N=3
Y0 = -(1. + N*XB)*ALOG(A)
DO 3 I=1,200
XA = 20.*I
OMEGAC3 = 1./(1. + 3.*(XB + XA))
PD3 = (1./((1. - OMEGAC3)**2))*EXP(-OMEGAC3*Y0)
WRITE(10,*) PD3,10.*ALOG10(XA)
C   WRITE(*,*) PD3,10.*ALOG10(XA)
3 CONTINUE
RETURN
END

```



```

C
C   PDF FOR THE COMPOUND-K
C
EXTERNAL FUNCTION BESSK1
OPEN(UNIT=10,FILE='C:\tecplot\compound.dat')
OPEN(UNIT=11,FILE='C:\tecplot\rayleigh.dat')
OPEN(UNIT=12,FILE='C:\tecplot\approxim.dat')
PI = 3.1415926536
ALPHA = 1.
KAPPA = 1.
SIGMAC = SQRT(3.)/ALPHA
PWR1 = (1/2) + KAPPA
PWR2 = 2
DO 1 I=1,100
  FI = I
  X = FI*0.15
  COMPK = 4.*(ALPHA**PWR1)*(X**PWR2)*BESSK1(2.*SQRT(ALPHA)*X)
  WRITE(10,*) X,COMPK
1 CONTINUE
DO 2 J=1,100
  FJ = J
  XX = FJ*0.1
  RAYLEIGH = (XX/SIGMAC)*EXP(-XX**2/(2.*SIGMAC))
  WRITE(11,*) XX,RAYLEIGH
2 CONTINUE
PWR1 = KAPPA + 0.5
DO 3 K=1,100
  FK = K
  XG = 0.1*FK
  APPROX = 2.*SQRT(PI)*XG**PWR1*EXP(-2.*XG)
  WRITE(12,*) XG,APPROX
  WRITE(*,*) XG,APPROX
3 CONTINUE
STOP
END

```

```

C
C   CALCULATE THE RICE PDF
C
EXTERNAL FUNCTION BESSIO
OPEN(UNIT=10,FILE='C:\fortran\probrilty\code\ricepdf.out')
OPEN(UNIT=11,FILE='C:\fortran\probrilty\code\gausspdf.out')
OPEN(UNIT=12,FILE='C:\fortran\probrilty\code\swerlpdf.out')
X=0.01
XRCS = 1.
SIGMA = 0.4
PI = 3.1415926536
DO 1 I=1,101
  FI = I
  Y = (FI-1.)*.1
  Z = X*Y
  R1 = BESSIO(2.*SQRT(Z))
  R2 = exp(-(X+Y))*R1
  R3 = (1./(SIGMA*SQRT(2.*PI)))*EXP(-(Y**2/(2.*SIGMA**2)))
  R4 = (1./XRCS)*EXP(-Y/XRCS)
  WRITE(10,*) Y,R2
  WRITE(11,*) Y,R3
  WRITE(12,*) Y,R4
1 CONTINUE
STOP
END

FUNCTION bessio(x)
REAL bessio,x
REAL ax
DOUBLE PRECISION p1,p2,p3,p4,p5,p6,p7,q1,q2,q3,q4,q5,q6,q7,q8,q9,y
SAVE p1,p2,p3,p4,p5,p6,p7,q1,q2,q3,q4,q5,q6,q7,q8,q9
DATA p1,p2,p3,p4,p5,p6,p7/1.0d0,3.5156229d0,3.0899424d0,
*1.2067492d0,0.2659732d0,0.360768d-1,0.45813d-2/
DATA q1,q2,q3,q4,q5,q6,q7,q8,q9/0.39894228d0,0.1328592d-1,
*0.225319d-2,-0.157565d-2,0.916281d-2,-0.2057706d-1,0.2635537d-1,
*-0.1647633d-1,0.392377d-2/
if (abs(x).lt.3.75) then
  y=(x/3.75)**2
  bessio=p1+y*(p2+y*(p3+y*(p4+y*(p5+y*(p6+y*p7))))))
else
  ax=abs(x)
  y=3.75/ax
  bessio=(exp(ax)/sqrt(ax))*(q1+y*(q2+y*(q3+y*(q4+y*(q5+y*(q6+y*
*(q7+y*(q8+y*q9))))))))
endif
return
END
C (C) Copr. 1986-92 Numerical Recipes Software i_91y.

```

```

C
C  CALCULATE PROBABILITY OF FALSE ALARM
C
EXTERNAL F
EXTERNAL G
EXTERNAL FACTLN
COMMON/POWER/ N
OPEN(UNIT=10,FILE='C:\fortran\probiilty\data\data.in')
OPEN(UNIT=11,FILE='C:\fortran\probiilty\code\falsealarm.out')
READ(10,*) CLTRNOIS,AK,N
DO 1 I=1,101
  FI = I
  TON = (FI-1.)*0.05
  R1 = EXP(-TON)
  R2 = CLTRNOIS*(AK**2)*(AK+1.)*(AK+2.)/(AK**4 + 3.*(AK**3)
x    -2.*AK + 1.)
  CALL TRAP(F,TON,20.,ANS1,10)
  CALL TRAP(G,TON,20.,ANS2,10)
  R3 = FACTRL(N)
  R4 = ANS1/R3
  R5 = (N**2)*R2*ANS1/R3
  R6 = -N*R2*ANS2/R3
  PFA = R4 + R5 + R6
  IF(PFA .GE. 0.) THEN
    PFA = PFA
  ELSE
    PFA = 0.
  ENDIF
  WRITE(*,*) PFA
  WRITE(11,*) TON,PFA
1 CONTINUE
STOP
END

FUNCTION F(X)
COMMON/POWER/ N
F = (X**(N-1))*EXP(-X)
RETURN
END

FUNCTION G(X)
COMMON/POWER/ N
G = (X**N)*EXP(-X)
RETURN
END

```

```

FUNCTION factrl(n)
  INTEGER n
  REAL factrl
CU  USES gammln
  INTEGER j,ntop
  REAL a(33),gammln
  SAVE ntop,a
  DATA ntop,a(1)/0,1./
  if (n.lt.0) then
    pause 'negative factorial in factrl'
  else if (n.le.ntop) then
    factrl=a(n+1)
  else if (n.le.32) then
    do 11 j=ntop+1,n
      a(j+1)=j*a(j)
11  continue
    ntop=n
    factrl=a(n+1)
  else
    factrl=exp(gammln(n+1.))
  endif
  return
END
C (C) Copr. 1986-92 Numerical Recipes Software i_91y.

```

```

FUNCTION gammln(xx)
  REAL gammln,xx
  INTEGER j
  DOUBLE PRECISION ser,stp,tmp,x,y,cof(6)
  SAVE cof,stp
  DATA cof,stp/76.18009172947146d0,-86.50532032941677d0,
    *24.01409824083091d0,-1.231739572450155d0,.1208650973866179d-2,
    *-.5395239384953d-5,2.5066282746310005d0/
  x=xx
  y=x
  tmp=x+5.5d0
  tmp=(x+0.5d0)*log(tmp)-tmp
  ser=1.000000000190015d0
  do 11 j=1,6
    y=y+1.d0
    ser=ser+cof(j)/y
11  continue
  gammln=tmp+log(stp*ser/x)
  return
END
C (C) Copr. 1986-92 Numerical Recipes Software i_91y.

```

```

SUBROUTINE trap(F,a,b,s,n)
INTEGER n
REAL a,b
REAL S,F,SUM
EXTERNAL F
INTEGER it,j
REAL del,tnm,x
if (n.eq.1) then
  s=0.5*(b-a)*(F(a)+F(b))
else
  it=2**(n-2)
  tnm=it
  del = (b-a)/tnm
  x = a + 0.5*del
  sum = 0.
  do 11 j=1,it
    sum = sum + F(x)
    x=x+del
11  continue
  s=0.5*(s+(b-a)*sum/tnm)
endif
return
END
C (C) Copr. 1986-92 Numerical Recipes Software i_91y.

```

```

FUNCTION bessk1(x)
REAL bessk1,x
CU  USES bessil
REAL bessil
DOUBLE PRECISION p1,p2,p3,p4,p5,p6,p7,q1,q2,q3,q4,q5,q6,q7,y
SAVE p1,p2,p3,p4,p5,p6,p7,q1,q2,q3,q4,q5,q6,q7
DATA p1,p2,p3,p4,p5,p6,p7/1.0d0,0.15443144d0,-0.67278579d0,
*-0.18156897d0,-0.1919402d-1,-0.110404d-2,-0.4686d-4/
DATA q1,q2,q3,q4,q5,q6,q7/1.25331414d0,0.23498619d0,-0.3655620d-1,
*0.1504268d-1,-0.780353d-2,0.325614d-2,-0.68245d-3/
if (x.le.2.0) then
  y=x*x/4.0
  bessk1=(log(x/2.0)*bessil(x))+(1.0/x)*(p1+y*(p2+y*(p3+y*(p4+y*
*(p5+y*(p6+y*p7))))))
else
  y=2.0/x
  bessk1=(exp(-x)/sqrt(x))*(q1+y*(q2+y*(q3+y*(q4+y*(q5+y*(q6+y*
*q7))))))
endif
return
END
C (C) Copr. 1986-92 Numerical Recipes Software i_91y.

```

```

FUNCTION bessil(x)

```

```

REAL bessl0,x
REAL ax
DOUBLE PRECISION p1,p2,p3,p4,p5,p6,p7,q1,q2,q3,q4,q5,q6,q7,q8,q9,y
SAVE p1,p2,p3,p4,p5,p6,p7,q1,q2,q3,q4,q5,q6,q7,q8,q9
DATA p1,p2,p3,p4,p5,p6,p7/1.0d0,3.5156229d0,3.0899424d0,
*1.2067492d0,0.2659732d0,0.360768d-1,0.45813d-2/
DATA q1,q2,q3,q4,q5,q6,q7,q8,q9/0.39894228d0,0.1328592d-1,
*0.225319d-2,-0.157565d-2,0.916281d-2,-0.2057706d-1,0.2635537d-1,
*-0.1647633d-1,0.392377d-2/
if (abs(x).lt.3.75) then
  y=(x/3.75)**2
  bessl0=p1+y*(p2+y*(p3+y*(p4+y*(p5+y*(p6+y*p7))))
else
  ax=abs(x)
  y=3.75/ax
  bessl0=(exp(ax)/sqrt(ax))*(q1+y*(q2+y*(q3+y*(q4+y*(q5+y*(q6+y*
*(q7+y*(q8+y*q9))))))))
endif
return
END

```

C (C) Copr. 1986-92 Numerical Recipes Software i_91y.

```

FUNCTION bessl1(x)
REAL bessl1,x
REAL ax
DOUBLE PRECISION p1,p2,p3,p4,p5,p6,p7,q1,q2,q3,q4,q5,q6,q7,q8,q9,y
SAVE p1,p2,p3,p4,p5,p6,p7,q1,q2,q3,q4,q5,q6,q7,q8,q9
DATA p1,p2,p3,p4,p5,p6,p7/0.5d0,0.87890594d0,0.51498869d0,
*0.15084934d0,0.2658733d-1,0.301532d-2,0.32411d-3/
DATA q1,q2,q3,q4,q5,q6,q7,q8,q9/0.39894228d0,-0.3988024d-1,
*-0.362018d-2,0.163801d-2,-0.1031555d-1,0.2282967d-1,-0.2895312d-1,
*0.1787654d-1,-0.420059d-2/
if (abs(x).lt.3.75) then
  y=(x/3.75)**2
  bessl1=x*(p1+y*(p2+y*(p3+y*(p4+y*(p5+y*(p6+y*p7))))
else
  ax=abs(x)
  y=3.75/ax
  bessl1=(exp(ax)/sqrt(ax))*(q1+y*(q2+y*(q3+y*(q4+y*(q5+y*(q6+y*
*(q7+y*(q8+y*q9))))))))
  if(x.lt.0.)bessl1=-bessl1
endif
return
END

```

C (C) Copr. 1986-92 Numerical Recipes Software i_91y.

REPORT DOCUMENTATION PAGE

Form Approved
OMB No. 0704-0188

Public reporting burden for this collection of information is estimated to average 1 hour per response, including the time for reviewing instructions, searching existing data sources, gathering and maintaining the data needed, and completing and reviewing the collection of information. Send comments regarding this burden estimate or any other aspect of this collection of information, including suggestions for reducing this burden, to Washington Headquarters Services, Directorate for Information Operations and Reports, 1215 Jefferson Davis Highway, Suite 1204, Arlington, VA 22202-4302, and to the Office of Management and Budget, Paperwork Reduction Project (0704-0188), Washington, DC 20503.

1. AGENCY USE ONLY (Leave blank)		2. REPORT DATE January 1997		3. REPORT TYPE AND DATES COVERED Final November 1996	
4. TITLE AND SUBTITLE TARGET DETECTION IN WIDEBAND CLUTTER AND NOISE CLOSED-FORM DETECTION ALGORITHMS FOR RADAR SYSTEM MODELING				5. FUNDING NUMBERS C: N66001-D-94-0009 PE: 0602232N AN: DN305339 WU: SXBD	
6. AUTHOR(S) R. H. Ott, GRCI, Inc.; D. R. Wehner, QuestTech, Inc.; R. J. Dinger, NRaD					
7. PERFORMING ORGANIZATION NAME(S) AND ADDRESS(ES) QuesTech, Inc. 1011 Camino del Rio South, Ste 600 San Diego, CA 92108 GRCI, Inc. 3900 Juan Tabo Blvd., NE, Ste 12 Albuquerque, NM 87111-3984				8. PERFORMING ORGANIZATION REPORT NUMBER NRaD TD 2940	
9. SPONSORING/MONITORING AGENCY NAME(S) AND ADDRESS(ES) Naval Command, Control and Ocean Surveillance Center RDT&E Division San Diego, CA 92152-5001				10. SPONSORING/MONITORING AGENCY REPORT NUMBER	
11. SUPPLEMENTARY NOTES					
12a. DISTRIBUTION/AVAILABILITY STATEMENT Approved for public release; distribution is unlimited.				12b. DISTRIBUTION CODE	
13. ABSTRACT (Maximum 200 words) This work derived the mathematics required in the Radar Simulation Concept Evaluation Model (RSCem) for closed-form answers for the probability of detection and false alarm for Swerling class targets in clutter and noise and targets in compound-K clutter plus noise. In all cases, the results are applicable to the N-pulse coherent detection problem. For the case of a target in "spikey" clutter plus the noise, the advantage of multiple pulse integration is significant.					
14. SUBJECT TERMS Mission area: Surveillance target detection probability theory radar clutter Gaussian noise radar detection compound-K pdf					15. NUMBER OF PAGES 83
					16. PRICE CODE
17. SECURITY CLASSIFICATION OF REPORT UNCLASSIFIED	18. SECURITY CLASSIFICATION OF THIS PAGE UNCLASSIFIED	19. SECURITY CLASSIFICATION OF ABSTRACT UNCLASSIFIED	20. LIMITATION OF ABSTRACT SAME AS REPORT		

21a. NAME OF RESPONSIBLE INDIVIDUAL R. J. Dinger	21b. TELEPHONE <i>(include Area Code)</i> (619) 553-2500	21c. OFFICE SYMBOL Code D755

INITIAL DISTRIBUTION

Code D0012	Patent Counsel	(1)
Code D0271	Archive/Stock	(6)
Code D0274	Library	(2)
Code D0271	D. Richter	(1)
Code D702	K. J. Campbell	(1)
Code D705	R. M. Niski	(1)
Code D755	R. J. Dinger	(10)
Code D8505	J. W. Rockway	(1)
Code D88	J. H. Richter	(1)
Code D882	H. V. Hitney	(1)
Code D883	W. L. Patterson	(1)

Defense Technical Information Center
Fort Belvoir, VA 22060-6218 (4)

NCCOSC Washington Liaison Office
Washington, DC 20363-5100

Center for Naval Analyses
Alexandria, VA 22302-0268

Navy Acquisition, Research and Development
Information Center (NARDIC)
Arlington, VA 22244-5114

GIDEP Operations Center
Corona, CA 91718-8000

Office of Naval Research
Arlington, VA 22217 (6)

Naval Postgraduate School
Monterey, CA 93943 (2)

Naval Research Laboratory
Washington, DC 20375-5320 (3)

Program Executive Officer
Theater Air Defense
Arlington, VA 22242-5170 (3)

Naval Surface Warfare Center
Dahlgren Division
Dahlgren, VA 22448-5100

Army Research Laboratory
Adelphi, MD 20783

Naval Air Warfare Center
Weapons Division
China Lake, CA 93555-6001 (3)

Sandia National Laboratories
Albuquerque, NM 87185

Metron, Inc.
Calabasa, CA 91372

SRI International
Menlo Park, CA 94025 (2)

Codar Ocean Sensors, Ltd.
Los Altos, CA 94024

University of Illinois at Chicago
Chicago, IL 60608

Dynamics Technology, Inc.
Torrance, CA 90503-2117

Dynamics Technology, Inc.
Arlington, VA 22209

(2)

SUNY Buffalo
Amherst, NY 14260

Applied Physics Laboratory
Laurel, MD 20723

(5)

Ohio State University
Columbus, OH 43212

Sanders (Lockheed-Martin)
Nashua, NH 03061

GRCI, Inc.
SWL Division
Vienna, VA 22182

Institute for Defense Analysis
Alexandria, VA 22311

GRCI, Inc.
Santa Barbara, CA 93111

PAR Government Systems Corporation
La Jolla, CA 92037

U. S. Department of Commerce
Boulder, CO 80303

DARPA
Arlington, VA 22203